Langevin fluctuation–dissipation fission dynamics of excited nuclei

I. I. Gonchar
Omsk State Railway Academy, 644046 Omsk

Fiz. Élem. Chastits At. Yadra **26**, 932–1000 (July–August 1995)

Dynamical models of the fission of compound nuclei formed in heavy-ion complete fusion reactions are reviewed. In these models, the emission of light particles and γ rays, which competes with fission and accompanies it, has an important influence. In these models, the fission process is treated as the random walk of an imaginary Brownian particle in the space of collective variables. The most important physical effects are the fluctuations of these variables and energy dissipation. Stochastic equations of the type of the classical Langevin equation are used as dynamical equations. Various questions that require urgent solution in connection with the development of such models are identified. The main attention is devoted to the so-called combined dynamical–statistical model, since it has been used up to the present time in the investigation of more experimental data than in all the other models of this type taken together. This analysis has made it possible to clarify which of the observables carry the most complete information about the dissipative properties of the fission mode and to propose several new experiments. © *1995 American Institute of Physics.*

INTRODUCTION

In any branch of physics, the concept of "dissipation" appears immediately and naturally after the division of the degrees of freedom of the system into collective (slow) and internal (fast, over which averaging is performed) variables. On general grounds, one could have expected intensive use of this concept in nuclear physics immediately after the fission reaction, discovered by Hahn and Strassmann in 1938 (the events of those years are described in Hilscher's review[1]), had been explained by Bohr and Wheeler on the basis of liquid-drop ideas.[2] However, the success of the statistical model in interpreting the experimental data delayed the investigation of the dissipative properties of nuclei in the fission process for 30–40 years, so that the first theoretical[3,4] and experimental[5,6] studies on this subject remained unused for a long time. The concept of dissipation began to be used intensively in nuclear physics in the first place through the discovery of deep inelastic collisions of heavy ions[7,8] and only in the last 10–15 years became established in fission physics.

This "reanimation" of dissipation in fission physics began at the end of the seventies and the beginning of the eighties with the studies of Nix and his collaborators on the mean kinetic energies of fission fragments[9,10] and with the studies of Weidenmüller and collaborators, who analyzed the effect of friction on the width of the distribution of the fission fragments with respect to the total kinetic energy.[11,12] The proposed approach was generalized to the case of several collective degrees of freedom by Adeev and collaborators[13,14] and was successfully used by this group to describe the experimentally observed variances of the mass,[15,16] energy,[17,18] and charge[19] distributions of the fragments (so-called diffusion model or fluctuation–dissipation dynamics of formation of the fission-fragment distributions).

Simultaneously, Weidenmüller and his collaborators analyzed the influence of friction on the fission rate[20,21] and demonstrated[22,23] that dissipative effects can lead to the emission of a greater number of neutrons from a fissioning nucleus than is predicted by the equilibrium statistical model. In the middle of the eighties, there was published a large amount of experimental data[24–27] that appeared to confirm qualitatively the conclusions of the theoretical studies of Refs. 22 and 23.

However, the problem of dissipation in the fission process proved to be much more complicated than appeared initially. The currently existing theoretical models predict a value of the damping coefficient for the fission mode β from 10^4–10^2 (Ref. 28) to 2–6 (Refs. 29 and 30) in units of 10^{21} s^{-1} (a systematization of the theoretical values of β is given in the review of Hilscher and Rossner[31]). The dependence of the nuclear viscosity on the temperature also varies very widely: from approximately direct proportionality (with increasing β from $0.4\cdot10^{21}$ s^{-1} at $T=0.5$ MeV to $7.6\cdot10^{21}$ s^{-1} at $T=4$ MeV)[32] to an inverse proportionality to the square of the temperature, as it should be for a Fermi liquid.[33]

The situation is complicated by the fact that nuclear friction is not an experimentally observable quantity and must be extracted from data. We mention first the experimental data on the energy distributions of the fission fragments,[34–38] on which great hopes were place in this regard. However, theoretical investigations extending over many years (Refs. 9, 10, 17, 18, and 39–44) showed that the strong dependence of the calculated kinetic energies on the criteria of division of a nucleus into two fragments does not make it possible to deduce the type and magnitude of nuclear friction from the data. We shall not return to this question, since it would increase the length of the review too much.

The data on light particles emitted by a fissioning nucleus form another group. Information about nuclear friction can also be extracted from these data only by means of complicated theoretical models. Until recently, systematic analysis of the experimental data had been done almost exclusively by means of the statistical model, into which more

 1063-7796/95/040394-29$10.00

or less arbitrary modifications were introduced in order to model the influence of friction on the fission process. Only recently have there appeared dynamical models that take into account the effect of dissipation and the fluctuations in a self-consistent manner.

The aim of this paper is to give a critical review of these models and to identify some questions that require urgent solution. The main attention will be devoted to the so-called combined dynamical–statistical model, not only because the author participated in its development but, mainly, because in the framework of this model more experimental data have been analyzed than by means of all the remaining models of this type taken together.

In their dynamical aspect, the models that we are considering are based on a picture of the fission process as the random walk of an imaginary Brownian particle in the space of collective variables. Therefore, in Sec. 1, which is mainly devoted to an analysis of the status of the problem at the end of the eighties, we also discuss the mathematical formalism used to describe a Markov process in a closed system.

In Sec. 2, we describe the combined dynamical–statistical model (CDSM), which combines Langevin fluctuation–dissipation dynamics with the standard statistical model. We discuss in detail the matching of the dynamical and statistical branches of this model.

Section 3 contains an analysis of the mean multiplicities of prescission neutrons and the fission probabilities made by means of the CDSM. We find here a set of parameters of the model, called for brevity the standard parameter set, by means of which it has proved possible to describe the experimental data in a wide range of the fissility parameter and the excitation energy of the compound nucleus.

In Sec. 4, we present the results of an analysis of the spectra and multiplicities of prescission charged particles and γ rays, the time distributions of the fission events, and the excitation energies of the nuclei at the scission point. Here some theoretical predictions are made, and some experiments are proposed.

1. STATUS OF THE PROBLEM

1.1. Diffusion model and its use to describe the fission process

In the diffusion model (Refs. 13–19 and 43–47), the fission process is described by means of several collective variables, which usually correspond to the main deformation modes. This system, which has a small number of degrees of freedom and can be conveniently called the *particle*, interacts with the large number of remaining (mainly single-particle) degrees of freedom of the nucleus, the detailed information about which does not interest us. In such a case, the dynamics of the collective variables is similar to the dynamics of a Brownian particle, since in one interaction event with the heat bath the energy of the particle changes little. The situation differs from ordinary Brownian motion in that the fluctuations in the energy of the particle have a significant influence on the energy of the "heat bath," so that its main characteristic—the temperature—becomes a function of the collective variables.

The basic equation of the diffusion model is the Fokker–Planck equation, which can be written in the form

$$\frac{\partial}{\partial t} P(\xi,t)=L(\xi)P(\xi,t), \tag{1}$$

where the Fokker–Planck operator has the form

$$L(\xi)=-\frac{\partial}{\partial \xi_i}\Phi_i(\xi)+\frac{\partial^2}{\partial \xi_i \partial \xi_j} D_{ij}(\xi). \tag{2}$$

Here ξ is the vector of the collective coordinates and momenta, Φ_i are drift coefficients, and D_{ij} is the symmetric tensor of the diffusion coefficients. Unless stated otherwise, summation over repeated indices is understood everywhere. The Latin indices take values from 1 to $2s$ (s is the number of degrees of freedom of the particle). In fission, the drift coefficients are usually associated with the right-hand sides of the classical (i.e., without allowance for the fluctuations) dissipative equations of motion for the collective momenta,

$$\Phi_\gamma(\xi)=\dot{p}_\gamma=-\frac{1}{2}\mu_{\beta\delta,\gamma}p_\beta p_\delta - V_{,\gamma}-\eta_{\beta\gamma}\mu_{\beta\omega}p_\omega, \tag{3}$$

and coordinates,

$$\Phi_{2S+\gamma}(\xi)=\dot{q}_\gamma=\mu_{\beta\gamma}p_\beta. \tag{4}$$

Here the Greek indices take values from 1 to s, and the dependence on the collective coordinates for the friction ($\eta_{\beta\gamma}$) and inverse inertial ($\mu_{\beta\gamma}$) parameters, and also for the potential energy V is not explicitly indicated. The index after a comma indicates differentiation with respect to the given variable. The inertial parameters $m_{\beta\gamma}$, in terms of which the matrix of the inverse inertial parameters is expressed, are usually calculated for excited nuclei by means of the Werner–Wheeler method[9] in the hydrodynamic approach. It is assumed that the friction parameters are related to the diffusion parameters by Einstein's relations:

$$D_{\beta\gamma}(\xi)=\eta_{\beta\gamma}(\mathbf{q})T(\xi). \tag{5}$$

Through the level-density parameter a, the temperature T is related to the internal excitation energy by the relation of the Fermi-gas model:

$$T(\xi)=(E^*/a)^{1/2}, \tag{6}$$

in which the internal excitation energy E^* is determined by the initial (total) excitation energy E^*_{tot}, and also by the potential, $V(\mathbf{q})$, and kinetic, $E_{\text{kin}}(\xi)$, energies of the collective degrees of freedom:

$$E^*=E^*_{\text{tot}}-V(\mathbf{q})-E_{\text{kin}}(\xi). \tag{7}$$

It is well known that the Fokker–Planck equation is equivalent to a system of stochastic Langevin equations (see Refs. 48–50). In the case of one degree of freedom, which is the most interesting for us, the Langevin equations have the form

$$\dot{q}=\frac{p}{m};\quad \dot{p}=-\beta p-\frac{dV}{dq}+\tilde{b}(t), \tag{8}$$

where p is the collective momentum conjugate to the coordinate q, β is the damping coefficient ($\beta=\eta/m$; η is the friction parameter), and $\tilde{b}(t)$ is a δ-correlated random force:

$$\langle \tilde{b}(t)\rangle = 0; \quad \langle \tilde{b}(t_1)\tilde{b}(t_2)\rangle = 2\eta T\delta(t_1 - t_2). \tag{9}$$

The first study in which Langevin equations were used to describe fission was purely methodological in nature and was published by Abe and collaborators in 1986.[51] They showed that numerical modeling for a free Brownian particle gives a result in agreement with the well-known analytic solution.[50] They also calculated the flux of particles through the barrier—the *fission rate*—and showed that its numerical value agrees with Kramers's formula (23). We shall call such an approach to the description of the process Langevin fluctuation–dissipation dynamics (LFDD).

In the years 1988–92, Langevin equations were intensively used by Fröbrich and collaborators[52–56] to describe collisions and fusion of heavy ions. They obtained a satisfactory description of the experimental data on the cross sections of deep inelastic collisions and fusion, and also on the distribution of the compound nuclei with respect to the spin; moreover, in a number of cases the theoretical analysis made it possible to find inaccuracies in the normalization of the experimental data (see Ref. 55).

An important dimensionless parameter that determines the nature of the solution of the system (8) is the ratio

$$\tilde{\beta} = \beta/(2\omega), \tag{10}$$

with collective "frequency"

$$\omega = \sqrt{\frac{1}{m}\frac{d^2V(q)}{dq^2}}. \tag{11}$$

In the case $\tilde{\beta} > 1$, the motion has the nature of aperiodic damping ("overdamping"). In this process, the momentum relaxes rapidly (during a time β^{-1}), whereas a much longer time, of the order of $\beta\omega^{-2}$, is required for the relaxation of the coordinate. If we are not interested in "fast" (in the indicated sense) processes, the dynamics of the Brownian particle can be described by the single Langevin equation

$$\frac{dq}{dt} = -\frac{1}{\eta}\left(\frac{dV}{dq}\right) + \sqrt{T/\eta}\,b(t). \tag{12}$$

Here $b(t)$ has the same meaning as $\tilde{b}(t)$. We shall call this equation, which in the diffusion model corresponds to Smoluchowski's equation, the *reduced* Langevin equation (RLE). The step in the integration of the RLE increases with increasing friction, and this permits a strong economization on computer time.

The Fokker–Planck equation describing the Markov process is the zeroth approximation in the relaxation time τ_{ther} of the heat bath, which is equal to the correlation time of the random force. The extent to which such an approximation is good for a particular collective mode can be gauged by comparing τ_{ther} with the characteristic time (relaxation time) of that mode, τ_{coll}. Qualitative estimates lead to the relation

$$\frac{\tau_{\text{ther}}}{\tau_{\text{coll}}} \approx \frac{1}{\sqrt{A}}, \tag{13}$$

which for medium and heavy nuclei gives a good small parameter of order 0.1. Calculations of τ_{ther} were made in Ref. 57 in the framework of linear-response theory. The length of the nucleus along the symmetry axis was taken as the collective variable. The time τ_{ther} was found to be in the range $(0.2–0.3)\cdot 10^{-21}$ s. This result justifies the use of the Fokker–Planck equation to describe the fission of excited nuclei. On the other hand, a Langevin equation for fission was recently derived microscopically from the so-called Boltzmann–Langevin equation by Ayik and collaborators.[58] This equation differs from the usual Boltzmann equation by the presence of an additional fluctuating term in the collision term. The resulting Langevin equation is of non-Markov type, and the time τ_{ther} is determined by

$$\frac{1}{\tau_{\text{ther}}} = 8\sigma v_{\text{F}} n\left(\frac{T}{\varepsilon_{\text{F}}}\right)^2, \tag{14}$$

where σ is the nucleon scattering cross section, v_{F} and ε_{F} are, respectively, the Fermi velocity and Fermi energy, and n is the number of particles per unit volume. In Ref. 59, in which these parameters were given the values $\sigma = 5$ F, $\varepsilon_{\text{F}} = 37$ MeV, $n = 0.16$ F^{-3}, the relaxation time of the heat bath was estimated at $\tau_{\text{ther}} = 2.6/T^2$ MeV$^2 10^{-21}$ s, which for $T = 1–2$ MeV leads to much larger numerical values than the result of Ref. 57.

Thus, the situation with regard to the applicability of the Markov description remains undecided. Practically all the results of the diffusion model that have hitherto been compared with experimental data were obtained by means of a Fokker–Planck equation, and "memory" effects were ignored.

1.2. Competition between fission and particle emission

The decay of excited nuclei through any channel is a purely fluctuation process, but the dynamics of the fluctuations is probably important only for the fission mode. A correct description of the competition between fission and deexcitation by particle emission is, thus, a topical dynamical problem of fission. During the last five–seven years, effective experimental methods have been developed that make it possible to separate out from the complete set of light particles (neutrons, protons, α particles) detected in coincidence with fission events those that were emitted before the scission of the neck connecting the incipient fragments. Following Hilscher,[31] we shall call these *prescission* neutrons. The mean multiplicity of the prescission neutrons, $\langle n_{\text{pre}}\rangle$, is a measure of the timescale of the fission process—it is a kind of "nuclear clock."[31]

The standard apparatus that traditionally has been used in the theoretical analysis of nuclear deexcitation is the statistical model (it is described in Ref. 60 and analyzed critically in Ref. 61). However, at excitation energies $E^* > 70–90$ MeV calculations by means of this model led to values of $\langle n_{\text{pre}}\rangle$ below the experimental value.[25] A typical example of the dependence of $\langle n_{\text{pre}}\rangle$ on the energy of the projectile (experimental data and statistical calculation) is shown in Fig. 1. Note the "turning over" of the statistical curve, which, as we found in Ref. 63 and 64, is due to the spin distribution of the compound nuclei and is typical for reactions induced by heavy ions.

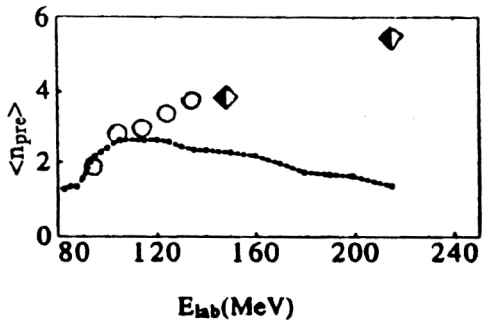

FIG. 1. Typical example of the dependence of $\langle n_{\rm pre}\rangle$ on $E_{\rm lab}$. The curve is our statistical calculation for the ^{28}Si+^{170}Er reaction. Experimental data: ^{28}Si+^{170}Er (○, Ref. 25); ^{20}Ne+^{181}Ta (half-filled diamonds, Ref. 62).

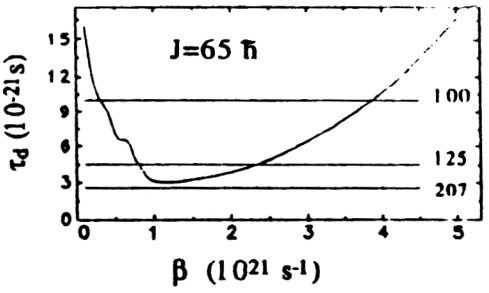

FIG. 2. Delay time as a function of β for the compound nucleus ^{158}Er at $E^*_{\rm tot}$ = 207 MeV and angular momentum 65$\hbar$. Also shown are the mean lifetimes until neutron emission $\langle t_n\rangle$ for several excitation energies (horizontal lines with numbers). The delay time depends weakly on the excitation energy [see Eqs. (16) and (17)]. The figure is constructed using Fig. 3 of Ref. 46 and Fig. 1 of Ref. 26.

Several attempts have been made to reproduce the observed dependence of $\langle n_{\rm pre}\rangle$ on E^* by means of the diffusion model (see Weidenmüller's review in Ref. 65, which we shall largely follow in this subsection, and also the original studies[26,46]). In the framework of this model, the *excess* neutrons (this is how we shall refer to the difference between the experimental value of $\langle n_{\rm pre}\rangle$ and the result obtained by the statistical calculation of this quantity) can be naturally explained by three physical effects:

1) emission in the process of establishment of a quasistationary probability flux through the fission barrier (characterized quantitatively by the *delay time* $\tau_{\rm d}$);

2) a decrease in the absolute value of this current due to viscosity (characterized quantitatively by

$$f_{\rm f}=\Gamma_{\rm f}/\Gamma_{\rm f}^{\rm BW}, \tag{15}$$

the inverse ratio of the Bohr–Wheeler fission width, $\Gamma_{\rm f}^{\rm BW}$ to the quasistationary fission width $\Gamma_{\rm f}$ with allowance for friction);

3) by the emission of neutrons on the path from the saddle point to the scission point (characterized quantitatively by the *time of descent* from the saddle to scission: $\tau_{\rm ss}$).

These effects will evidently be important if the characteristic time of neutron emission (the mean lifetime $\langle t_n\rangle$ with respect to decay through the neutron channel) is less than or of the order of $\tau_{\rm d}$ or $\tau_{\rm ss}$, and also if $f_{\rm f}$ is appreciably less than unity.

The delay time can be estimated from the relations[66]

$$\tau_{\rm d}\approx\beta(2\omega_{\rm gs}^2)^{-1}\ln(10B_{\rm f}/T) \tag{16}$$

for $\beta\gg 2\omega_{\rm gs}$ (overdamping) or

$$\tau_{\rm d}\approx\beta^{-1}\ln(10B_{\rm f}/T) \tag{17}$$

for $\beta\ll 2\omega_{\rm gs}$ (underdamping).

Here $\omega_{\rm gs}$ is the frequency of (undamped) vibrations near the potential-energy minimum of the fission mode, and $B_{\rm f}$ is the height of the fission barrier. The relations (16) and (17) are very general. For example, they can be used to calculate the relaxation time of the coordinate of the harmonic oscillator if the logarithmic factor is replaced by unity.[67] This factor is characteristic only of the class of problems under discussion (decay of a metastable state of a system through a barrier), and the numerical factor in the argument of the logarithm is a particular feature associated with the particular criterion of establishment of the quasistationary current through the fission barrier chosen in Refs. 65 and 66.

The behavior of $\tau_{\rm d}$ as a function of β is illustrated in Fig. 2. This shows the typical behavior of a relaxation time that is determined by competition between diffusion and dissipation. Figure 2 also shows the mean neutron emission times for different excitation energies. Comparison of $\tau_{\rm d}$ and $\langle t_n\rangle$ shows that the process of establishment of the quasistationary probability current through the fission barrier influences primarily the emission of the first neutron and does so at high excitation energies. Thus, one can hardly hope to explain the "deficit" of 2–3 neutrons in the statistical analysis (see, for example, Ref. 68) by the effect of the delay time.

The second dynamical factor, the decrease in the absolute value of the quasistationary probability current through the fission barrier due to viscosity, can be taken into account by introducing a correction factor $f_{\rm f}$ [see Eq. (15)]. This factor $f_{\rm f}$ has the form

$$f_{\rm f}=\frac{\left(\left(\omega_{\rm sd}^2+\frac{\beta^2}{4}\right)^{1/2}-\frac{\beta}{2}\right)}{\omega_{\rm sd}}\frac{\hbar\omega_{\rm gs}}{T} \tag{18}$$

for $\beta/\omega_{\rm gs}\geq T/B_{\rm f}$. For $\beta/\omega_{\rm gs}\leq T/B_{\rm f}$ (i.e., in the case of extremely weak friction), $f_{\rm f}$ takes the form

$$f_{\rm f}=\beta\frac{2\pi\hbar B_{\rm f}}{T^2}. \tag{19}$$

In accordance with the Bohr–Wheeler formula, the fission rate is

$$R_{\rm f}^{\rm BW}=\frac{1}{2\pi\hbar\rho_{\rm CN}(E^*_{\rm tot})}\int_0^{E^*_{\rm tot}-B_{\rm f}}d\varepsilon\,\rho_{\rm f}(E^*_{\rm tot}-B_{\rm f}-\varepsilon). \tag{20}$$

Here $\rho_{\rm CN}$ is the level density of the compound nucleus at the deformation corresponding to the ground state, and $\rho_{\rm f}$ is the level density of the compound nucleus at the fission barrier. We shall discuss the relationship between the Bohr–Wheeler expression and Kramers's expression for the quasistationary fission rate in more detail below. Here we merely note that the behavior of $(R_{\rm f}^{\rm K})^{-1}$ as a function of β is the same as that of $\tau_{\rm d}$ in Fig. 2, although the actual times may be very differ-

ent. This is natural, since the quasistationary decay of a metastable state is simply relaxation. In this sense, we may call τ_d the "relaxation time of the relaxation time."

The dynamical factor f_f has a strong effect not only on the multiplicity of the prescission neutrons but also on the final fission and survival probabilities. Therefore, in Ref. 46 it was necessary to introduce a β-dependent correction to the ratio a_f/a_n, where a_f is the density parameter of the single-particle levels in the fission channel (for the saddle deformation), and a_n is the density parameter of the single-particle levels in the neutron channel (for the ground state). However, this correction does not agree with the predictions of the theoretical models for the deformation dependence of the density of the single-particle levels (see, for example, Ref. 69).

Finally, a third dynamical factor is the descent time. It influences $\langle n_{pre}\rangle$ but does not affect the fission cross sections. Its importance increases for heavier fissioning nuclei and with increasing laboratory energy of the projectile for a given reaction. It is therefore to be expected that it will be this factor that is dominant in the experimentally observed growth of $\langle n_{pre}\rangle$ with increasing excitation energy in heavy-ion reactions. In reactions induced by light particles, the situation may be very different.

The diffusion model[46] was refined in Ref. 70 by Lanza and Weidenmüller, who took into account charged-particle emission accompanying fission. They investigated only the influence of the delay time on the mean multiplicity of prescission protons, $\langle p_{pre}\rangle$, in the fissioning of ^{152}Er at $E^*=140$ MeV, and the probability of fission after emission of an α particle was found to be vanishingly small. They found that the results of Ref. 46 for $\langle n_{pre}\rangle$ remain essentially unchanged, while the proton multiplicities do not exhibit such a strong dependence on the delay time as the neutron multiplicities. The conclusion of Ref. 70 is that $\langle p_{pre}\rangle$ can be used to determine the parameters of the statistical model more accurately but does not have independent value for the study of dissipative effects.

Completing our discussion of the series of studies of Weidenmüller and his collaborators, we note that the values of β at which it was possible to reproduce the experimental values of $\langle n_{pre}\rangle$ in Refs. 26 and 46 lie in the interval $(4-6)\times10^{21}$ s^{-1}. If the authors of Ref. 27 are correct, and the neutron multiplicities in the ^{16}O+^{142}Nd reaction are much greater than those published in Ref. 26, then the results of the analysis of Refs. 26 and 46 must be radically reconsidered.

The authors of Ref. 71 were the first to formulate a general approach to the mutual effect—the basis of the diffusion model—of the slow relaxation of the collective degrees of freedom and the emission of light particles on each other. They calculated the prescission multiplicities of neutrons, protons, and α particles for nuclei with $A\sim180$ at large angular momenta ($\sim40\hbar$) and high excitation energies ($T\sim5$ MeV). Such temperatures were achieved in heavy-ion reactions in GANIL.

We consider briefly some features of the model. The emission of particles in it is studied in the *continuous limit*, i.e., during a short time dt a small fraction of the total multiplicity of the particles of each species is emitted. These

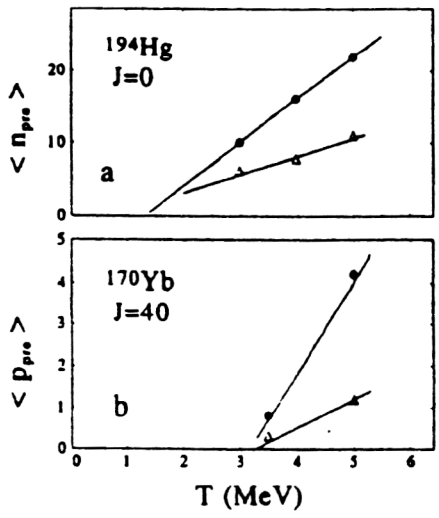

FIG. 3. Calculated dependences of $\langle n_{pre}\rangle$ (a) and $\langle p_{pre}\rangle$ (b) on the temperature (Ref. 71, Figs. 8a and 9b): dynamical calculation ●; statistical calculation △.

total multiplicities are then integrated, and the prescission multiplicities are constructed by means of the resulting functions of the time. The not too elegant but numerically very effective continuous limit has since been widely used in the literature.[40,42,43]

The diffusion model[71] was constructed for the overdamping regime. It was assumed that the distribution of the collective momenta relaxes to the equilibrium distribution, but a dependence of the friction and inertia parameters on the collective coordinate was allowed, even though the calculations were made only for β=const. Only the mean multiplicity of prescission neutrons was calculated, although in principle the diffusion model must give the distribution of the fission events with respect to the multiplicity of prescission neutrons. At temperatures of a few mega-electron-volts, the fissioning nucleus emits an appreciable number of neutrons and charged particles. Therefore, the temperature changes appreciably during the fission process, and it is necessary to take into account the temperature dependence of the liquid-drop "potential energy," as was done in Ref. 71 (we shall discuss this effect in detail below and define the terminology accurately there). In the diffusion model,[26,46] this effect was not taken into account.

Typical results of Ref. 71, taken from that study (Figs. 8a and 9b) are reproduced in Fig. 3. It can be seen that the increase of the prescission multiplicities in the dynamical calculation as compared with the statistical one is very appreciable, and the dependence of the dynamical curves agrees qualitatively with the experimental dependence. However, the same can also be said of the curves corresponding to the statistical calculation. Here the calculations were made for one partial wave, and there is not the decrease of $\langle n_{pre}\rangle$ at high excitation energies inherent in the complete statistical calculation with averaging over all partial waves. In Ref. 71, a quantitative comparison with experiment was not made.

Such a comparison was made in the framework of the

diffusion model in Ref. 47, and we conclude this subsection with a brief discussion of this study. As in Ref. 71, the continuous limit was used to describe the emission of particles. Calculations were made of the multiplicities of prescission neutrons, protons, and α particles, and also of their distribution with respect to the energy and angular momentum carried away. The formalism used in Ref. 47 also makes it possible to calculate the probabilities of fission and survival, the experimental data on which impose severe restrictions on the values of the model parameters. For example, there is consideration in Ref. 47 of a very wide spectrum of values of the coefficient that controls the dependence of the surface component of the potential energy on the temperature. This effect has a radical influence on the results, but the value of the coefficient was chosen arbitrarily, since a comparison of the theoretical results was made only with experimental data on $\langle n_{\text{pre}} \rangle$ in reactions for which data on the fission probability P_{f} were absent. The results of the analysis of the experimental data enabled the authors of Ref. 47 to establish only an upper limit on the damping coefficient: $\beta \leqslant 8 \cdot 10^{21}$ s^{-1}. Moreover, some of the data for analysis were taken from Ref. 26, and these data, like the data used in Ref. 46, do not fit the systematics of $\langle n_{\text{pre}} \rangle$.

1.3. Open problems

Thus, at the beginning of the nineties, several attempts were made in the framework of the diffusion model, which is based on the Fokker–Planck equation, to analyze the multiplicities of prescission neutrons (by Weidenmüller, Delagrange, Dietrich, and their collaborators: Refs. 20–23, 26, 46, 47, 65, 66, and 71). These studies, and also the work of Hilscher's group,[24] made it possible to establish that the collective nuclear damping with respect to the fission mode occurs in the overdamping regime. It was not possible to draw quantitative conclusions because of the contradictory nature of some experimental data (in particular, those of Refs. 26 and 27), but primarily on account of the imperfection of the theoretical models used for the analysis and the nonsystematic nature of the effect. A fairly complete impression of the spread of values of β extracted from the experiments is given by Table 4.2 in the review of Ref. 31.

Thus:

a) it was necessary to create a dynamical model permitting calculation of the distribution of fission events with respect to the number of emitted neutrons ("the fission chance"), which would permit the simultaneous analysis of the probabilities of fission and the multiplicity of prescission neutrons;

b) it was desirable to make such an analysis using the greatest number of data of different groups in order to eliminate the possibility of drawing conclusions based on incorrect data;

c) it was important to reduce to a minimum the number of independent adjustable parameters of the model and, in particular, to find restrictions on the coefficient that determines the temperature dependence of the surface energy (the very formulation of this problem was subject to doubt);

d) it would be helpful to find additional observables (besides $\langle n_{\text{pre}} \rangle$) sensitive to the fission dynamics.

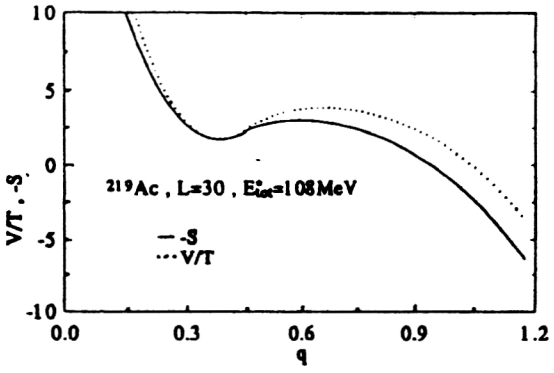

FIG. 4. Potential energy divided by the temperature (dotted curve) and the entropy with reversed sign and normalized to zero in the ground state of the nonrotating nucleus (continuous curve) as functions of the fission coordinate. The calculation was made for the ^{219}Ac nucleus at angular momentum $L=30$ and $E^*_{\text{tot}} = 108$ MeV (Ref. 78).

2. THE COMBINED DYNAMICAL–STATISTICAL MODEL (CDSM)[63,72–78]

2.1. The need to develop the one-dimensional LFDD and to construct the CDSM

The attempts to develop a consistent dynamical model of fission induced by heavy ions that included the emission of particles and γ rays encountered considerable difficulties.

In particular, the computing time required to model the trajectory of the Brownian particle making a random walk near the ground state at excitation energies somewhat greater than the height of the fission barrier exceeded all reasonable bounds. In addition, for very large times the problem of the stability of the solution arises. As a result, it was possible to study only systems having a 100% probability of fission during a comparatively short time. Physically, of course, the situation was much richer. However, since after a certain delay time the fissioning system reaches a quasistationary limit, further dynamical modeling becomes redundant: The regime of applicability of the statistical model is reached. In Ref. 72, it was therefore proposed to combine the LFDD with an appropriately modified statistical model.

For the purposes of describing the fission probability P_{f} and the multiplicity of prescission particles, it appeared sensible from the very beginning to restrict the dynamical treatment to a single degree of freedom, corresponding to the intercenter distance. The influence of the fission criterion on P_{f} was assumed to be minimal, since the system "takes the decision" whether or not to fission basically at the saddle point (transition-state method). The length of the path from the saddle to scission, which can significantly influence $\langle n_{\text{pre}} \rangle$, also depends weakly on the scission criterion (see, for example, Fig. 4 in the review of Ref. 39). The large number of neutrons emitted from the nucleus before scission at temperatures 1–3 MeV indicates that the fission motion is slow and takes place predominantly in the diffusion regime. Therefore, to describe the process it was decided to use the reduced Langevin equation corresponding to the overdamping regime. It was proposed to compensate these serious ap-

proximations by systematic analysis of the experimental material on the nucleon composition of the fissioning nuclei, their excitation energies, and with respect to several different observables.

2.2. Dynamical equation of the CDSM and the quasistationary fission rate

In this subsection, we discuss the formulas that lead to a consistent "matching" of the LFDD to the statistical model. We begin with the arguments for the need to modify the traditional approach (Refs. 39, 40, 43, 72, 79, and 80–84). For example, in Ref. 72 we used the RLE in the form (12). If this or any other dynamical equation is used, the fission rate can be calculated as

$$R_{\mathrm{f}}(t)=\frac{1}{(N_{\mathrm{tot}}-N_{\mathrm{f}}(t))}\frac{dN_{\mathrm{f}}(t)}{dt}, \tag{21}$$

by recording the number of Langevin trajectories $N_{\mathrm{f}}(t)$ that have reached the scission point in a time less than t; N_{tot} is the total number of trajectories.

In Ref. 72, after the transition from the dynamical to the statistical calculations, we used the Bohr–Wheeler expression for the fission width, modified by taking into account Kramers correction factor [see Eq. (8)]:

$$R_{\mathrm{f}}^{\mathrm{KBW}}=\frac{\omega_{\mathrm{sd}}\omega_{\mathrm{gs}}}{\beta T}R_{\mathrm{f}}^{\mathrm{BW}}. \tag{22}$$

This expression is written down for the case of overdamping. Here $R_{\mathrm{f}}^{\mathrm{BW}}$ is the standard Bohr–Wheeler expression for the fission rate[2] [see the expression (20)], the most important ingredients of which in the Fermi-gas model are the parameters a_n and a_{f}.

At times greater than the delay time, the fission rates calculated dynamically [in accordance with (21)] and statistically [in accordance with (22) for overdamping] must be equal. However, in the RLE (12) there is no information at all on the coordinate dependence of the level-density parameter, whereas it is precisely this dependence that determines the difference between a_n and a_{f} in the Bohr–Wheeler formula. As is well known, the ratio a_{f}/a_n is often used as an adjustable parameter in the statistical model to reproduce the data on the fission probabilities.[68,85–87] On the other hand, in the Bohr–Wheeler formula (20) there is no information at all about the scission point. Thus, we can expect agreement between the dynamical and statistical fission rates only if the coordinate dependence of the level-density parameter and the position of the scission point do not play any role.

In fact, $R_{\mathrm{f}}(t)$ are usually compared with the Kramers fission rate $R_{\mathrm{f}}^{\mathrm{K}}$ (Ref. 1):

$$R_{\mathrm{f}}^{\mathrm{K}}=f_{\mathrm{f}}\frac{T}{2\pi\hbar}e^{-B_{\mathrm{f}}/T}. \tag{23}$$

This expression can be obtained from (18) and (20) by using the Fermi-gas model [$\rho(E)\sim\exp(2\sqrt{aE})$ and $T=\sqrt{E_{\mathrm{tot}}^{*}/a}$] in the approximation $B_{\mathrm{f}}/E_{\mathrm{tot}}^{*}\ll 1$ and assuming that the level-density parameters in the ground state and at the saddle point are equal. Then

$$\begin{aligned}R_{\mathrm{f}}^{\mathrm{BW}}&=\frac{1}{2\pi\hbar\,\exp(2\sqrt{aE_{\mathrm{tot}}^{*}})}\\&\times\int_0^{E_{\mathrm{tot}}^{*}-B_{\mathrm{f}}}d\varepsilon\,\exp(2\sqrt{a(E_{\mathrm{tot}}^{*}-B_{\mathrm{f}}-\varepsilon)})\\&\simeq\frac{T}{2\pi\hbar}e^{-B_{\mathrm{f}}/T}.\end{aligned} \tag{24}$$

Comparisons of $R_{\mathrm{f}}(t)$ and $R_{\mathrm{f}}^{\mathrm{K}}$ were made in Refs. 51, 79, and 82, and the agreement was usually satisfactory. Moreover, it was shown in Ref. 79 that this agreement holds up to $B_{\mathrm{f}}/T>0.5$, whereas originally Kramers formula (23) was derived for the case $B_{\mathrm{f}}/T\gg 1$. Unfortunately, all the comparisons of Refs. 51, 79, and 82 were made for the case of a coordinate-independent level-density parameter and from a scission point lying far from the saddle point. Thus, the discrepancy between the dynamical and statistical descriptions of the fission rate remained unnoted for a long time.

However, it is well known that for the description of a heated nuclear system the potential energy in the dynamical equations must be replaced by the free energy $F(q,T)$ (Refs. 88–90). In the Fermi-gas model, which will be used throughout in what follows, the free energy is related to the level-density parameter as follows:

$$F(q,T)=V(q)-a(q)T^2. \tag{25}$$

A deformation dependence of the smooth part of the level-density parameter appears because of the presence of a gradient of the nucleon density on the nuclear surface[91] and is a general physical result.[92] Thus, information on the deformation dependence of the level-density parameter appears in the equation of motion, which takes the form

$$\frac{dq}{dt}=-\frac{1}{\eta}\left(\frac{\partial F}{\partial q}\right)\Big|_T+\sqrt{\left(\frac{T}{\eta}\right)}b(t). \tag{26}$$

The regular component of the force $K=-(\partial F/\partial q)|_T$ is now given by the derivative of the free energy with respect to the fission coordinate at constant temperature. Of course, the choice of a specific thermodynamic potential is a matter of taste.[93] In what follows, we shall take it to be the entropy $S(E_{\mathrm{tot}}^{*},q)$, which is a function of only q, since the total excitation energy $E_{\mathrm{tot}}^{*}(q,S)$ remains constant.

The total excitation energy is a sum of three terms: the kinetic energy E_{kin} of the collective motion, which in the case of overdamping is of the order of the nuclear temperature; the potential energy $V(q)$, and the internal excitation energy E^{*}. Using the relation $F=E_{\mathrm{tot}}^{*}-TS$ and ignoring E_{kin}, we obtain for the regular component of the force

$$K=-\partial F/\partial q|_T=T\partial S/\partial q|_{E_{\mathrm{tot}}^{*}}. \tag{27}$$

Since the nuclear system is closed, and E_{tot}^{*} remains constant, we use in what follows the total derivative with respect to the coordinate instead of the partial derivative:

$$T\left(\frac{\partial S}{\partial q}\right)\Big|_{E_{\mathrm{tot}}^{*}}=TdS/dq=TS'. \tag{28}$$

Then the reduced Langevin equation takes the form

$$\frac{dq}{dt}=\frac{T}{\eta}S'+\sqrt{\left(\frac{T}{\eta}\right)}b(t). \tag{29}$$

In the calculations whose results are discussed below, the Fermi-gas expression for the entropy was used:

$$S(q)=2\sqrt{a(q)(E^*_{\rm tot}-V(q))}. \tag{30}$$

One of the reasons why the entropy rather than the free energy is used in the CDSM is that, being normalized to zero in the ground state of the nucleus, the entropy plays the same role as $-V/T$. It is well known that the value of this ratio at the saddle point is the most important parameter of the standard statistical model.

In Ref. 63 a modified statistical expression for the fission rate, which must replace $R_{\rm f}^{\rm K}$, was derived. The derivation is based on the concept of the mean first passage time (MFPT), which is widely used in many branches of physics and chemistry (see, for example, Refs. 48–50 and 94). The value of the reciprocal MFPT is usually interpreted as the mean fission rate $R_{\rm MFPT}$:

$$R_{\rm MFPT}=\frac{T}{\eta}\left\{\int_{q_{\rm gs}}^{q_{\rm sc}}dy e^{-S(y)}\int_{-\infty}^{y}dz e^{S(z)}\right\}^{-1}. \tag{31}$$

This solution corresponds to an initial position $q_{\rm gs}$ of the particle in the ground state. The expression (31) generalizes to the case of heated closed systems the result obtained by Andronov, Pontryagin, and Vitt 60 years ago.[95]

Thus, the replacement of the potential by the entropy made it possible to derive a dynamical equation that contains information about the level-density parameter and an expression for the statistical fission rate that includes the position of the scission point. The inconsistency inherent in the expressions (12) and (22) used in Ref. 72 is eliminated by the replacement of them by (29) and (31), respectively.

In actual calculations, the use of the expression (31), which involves multiple calculation of a double integral for different A and Z, excitation energies, and angular momenta, would require unrealistically large amounts of computing time on the transition to the statistical branch of the model. To avoid this, we replace (31) by the approximate expression that is obtained by estimating the integrals by the method of steepest descent. Then the inner integration must be extended to infinity ($y\to\infty$), and in the outer integral we must set $q_{\rm gs}\to-\infty$. The resulting approximate expression for the fission rate is

$$R_{\rm app}=\frac{\tilde\omega_{\rm gs}\tilde\omega_{\rm sd}}{2\pi\beta}\exp[S(q_{\rm gs})-S(q_{\rm sd})]$$
$$\times 2(1+\mathrm{erf}\,[(q_{\rm sc}-q_{\rm sd})\tilde\omega_{\rm sd}\sqrt{m/2T}])^{-1}. \tag{32}$$

The saddle point and ground state are determined by the stationary points of the entropy and not by the potential energy, as in the usual approach. The frequencies $\tilde\omega_{\rm gs}=\sqrt{|S''|_{\rm gs}T/m}$ and $\tilde\omega_{\rm sd}=\sqrt{S''_{\rm sd}T/m}$ are now calculated in terms of the second derivatives of the entropy at the stationary point.

The influence of the scission point on the fission rate is also obvious from the expression (32). If the scission point is far from the saddle point, $\mathrm{erf}\,[(q_{\rm sc}-q_{\rm sd})\tilde\omega_{\rm sd}\sqrt{m/2T}]\to 1$. If the saddle point and scission point coincide, the error function tends to zero, and this leads to an increase of $R_{\rm app}$ by a factor 2 compared with the previous situation. The need to modify Kramers's formula if the saddle point and scission point are close to each other was noted by Strutinsky in Ref. 4.

Kramers's expression R_K (Ref. 3) for the case of overdamping can be obtained from (32) if the level-density parameter does not depend on the deformation, the scission point is far from the saddle point, and $E^*_{\rm tot}\gg V(q_{\rm sd})>V(q_{\rm gs})$:

$$R_{\rm K}=\frac{\omega_{\rm gs}\omega_{\rm sd}}{2\pi\beta}\exp\{(-V(q_{\rm sd})+V(q_{\rm gs}))/T\}, \tag{33}$$

where $\omega_{\rm gs}=\sqrt{V''_{\rm gs}/m}$ and $\omega_{\rm sd}=\sqrt{|V''|_{\rm sd}/m}$ are now related to the curvature of the potential energy at the stationary points.

In order to have the possibility of making systematic calculations of observables in a wide range of nuclei, it is necessary to develop an algorithm for rapid calculation of the potential energy and the level-density parameter as functions of the deformation. The following two subsections are devoted to these problems.

2.3. The potential energy[78]

Since we shall be mainly dealing with heated nuclei, shell corrections can be ignored. In the CDSM the liquid-drop set of parameters of Myers and Swiatecki[96] is used. The potential energy is given by

$$V(A,Z,L,q)=a_2(1-kI^2)A^{2/3}(B_s(q)-1)$$
$$+c_3\frac{Z^2}{A^{1/3}}(B_C(q)-1)$$
$$+c_r L^2A^{-5/3}B_r(q). \tag{34}$$

We have here omitted the terms that do not depend on the fission coordinate q. In accordance with Ref. 96, the parameters in (34) have the values

$$a_2=17.9439\ \text{MeV},\quad c_3=0.7053\ \text{MeV},$$
$$k=1.7826,\quad c_r=34.50\ \text{MeV}. \tag{35}$$

We do not take into account the corrections associated with the finite range of the nuclear forces, since we do not know a method for taking into account such corrections in the level-density parameter, and it is desirable to have the same order of accuracy in the potential energy and in the level-density parameter.

As in the previous section, we use the c,h,α parametrization[97] to calculate $B_s(q),B_C(q),B_r(q)$. We consider only the symmetric case ($\alpha=0$). In the case of overdamping, which is what we investigate, the system "slides" along the bottom of the fission valley, which then characterizes a one-dimensional potential. It turns out that the bottom of the fission valley of an individual nucleus passes near a sequence of saddle points of different nuclei. In the region in

which h_{sd} is a single-valued function of q_{sd}, it is possible to characterize B_s as a function of the deformation as follows:

$$B_s=\begin{cases}1+0.4\cdot 64/9\cdot(q-0.375)^2, & \text{if } q<0.452;\\ 0.983+0.439\cdot(q-0.375), & \text{if } q\geq 0.452;\end{cases} \tag{36}$$

To calculate B_C, we use the approximate expression by means of which the fission barrier B_f is expressed in terms of the fissility parameter X (Ref. 98):

$$\frac{B_f}{E_{ssp}}=\begin{cases}0.2599-0.2151X-0.1643X^2-0.0673X^3, & \text{if } X<0.6;\\ 0.7259Y^3-0.3302Y^4+0.6387Y^5 & \\ +7.8727Y^6-12.0061Y^7, & \text{if } X>0.6.\end{cases} \tag{37}$$

Here $Y=1-X$, and E_{ssp} is the surface energy of a spherical nucleus with fissility X. The dependence of the intercenter distance at the saddle point, q_{sd}, on the fissility parameter, which closes our one-dimensional parametrization of the potential energy for zero angular momentum, has the form

$$q_{sd}=0.375+\frac{0.875}{1+\exp(20(X-0.74))}. \tag{38}$$

The quantity $B_r(q)$ used in (34), is proportional to the reciprocal of the rigid-body moment of inertia. In the (c,h) parametrization, it is determined as

$$B_r=J_{\parallel}^{-1} \quad \text{if } J_{\perp}<J_{\parallel} \text{ and } q>0.375,$$

$$B_r=J_{\perp}^{-1} \quad \text{in all remaining cases;}$$

$$J_{\perp}=c^2\{1+c^{-3}+4B_{sh}[2c^3+(4/15)B_{sh}c^3-1]/35\}/2,$$

$$J_{\parallel}=c^2\{c^{-3}+4B_{sh}[(4/15)B_{sh}c^3-1]/35\}. \tag{39}$$

The nuclear shape parameter B_{sh} and our collective coordinate q can be expressed in terms of c and h as follows:

$$B_{sh}(c,h)=2h+(c-1)/2, \tag{40}$$

$$q(c,h)=\frac{3}{8}c\left(1+\frac{2}{15}B_{sh}c^3\right). \tag{41}$$

Our one-dimensional parametrization is not valid for very light nuclei, since $h_{sd}(q_{sd})$ and $q_{sd}(X)$ cease to be single-valued functions. Therefore, the parametrization works only if $X\geq 0.55$. However, this does not present too great difficulties in practical calculations, since light nuclei fission mainly at high angular momenta, which effectively increase the fissility parameter.

The parametrization described in this subsection makes it possible to perform calculations fairly rapidly for all cases of practical interest.

2.4. Parameter of the single-particle density of states and its dependence on the deformation[78]

For the adequate description of fission, the level-density parameter and its dependence on the deformation play a role that is as important as that of the potential energy. Ignoring the corrections for the curvature of the surface, we can express the smooth part of the single-particle level-density parameter in the form[92]

$$a(q)=\tilde{a}_1A+\tilde{a}_2A^{2/3}B_s(q). \tag{42}$$

Following Smirenkin and collaborators,[87] we chose among the many possibilities the weakest coordinate dependence that does not contradict the experimental data. It corresponds to the theoretical result of Ignatyuk and collaborators[91] obtained for the Woods–Saxon potential:

$$\tilde{a}_1=0.073 \text{ MeV}^{-1} \quad \text{and} \quad \tilde{a}_2=0.095 \text{ MeV}^{-1}. \tag{43}$$

It is interesting to note that in the cruder approximation of a rectangular or trapezoidal well the coefficient $\tilde{a}_2$ changes not only the absolute magnitude but even the sign.

In this section, we have the aim of constructing a self-consistent dynamical and statistical description of fission, and therefore the specific value of the coefficient $\tilde{a}_2$ plays no role. In contrast, in the following section, in which we compare the results of calculations with numerical data, the numerical value of $\tilde{a}_2$ will be extremely important.

Once we have chosen the parameters of the liquid-drop potential energy and the level-density parameter, the entropy S becomes a function of the mass and charge numbers, the angular momentum, the coordinate, and the total excitation energy:

$$S(\Lambda,Z,L,q,T)=2\sqrt{a(A,q)(E^*_{tot}-V(A,Z,L,q))}. \tag{44}$$

There are no further free adjustable parameters in either the dynamical or the statistical branch of the model except for the damping coefficient β, which occurs in both of them. It is natural to assume that this coefficient is universal for all nuclei. Thus, adjustable parameters of the type a_n, a_f/a_n, and B_f for *individual* nuclei are not present in our model, and we regard this as a serious advantage over the standard macroscopic statistical model.

2.5. Consistency of the dynamical and statistical descriptions of the fission rate[78]

We begin the discussion of the results with Fig. 4. Traditionally,[3,94] the fission rate is defined as the ratio of the difference of the potential energies at the saddle point and in the ground state to the temperature [see Eq. (33)], whereas in our approach this role is played by the difference of the corresponding entropies, as in the most refined form of the statistical model.[99] In Fig. 4, we therefore compare the potential energy $V(q)$, divided by the temperature, with the entropy taken with the opposite sign and normalized to zero at the ground state of the nonrotating nucleus for the example of ^{219}Ac. It can be seen that, compared with the potential energy, the entropy barrier is not only lowered but is

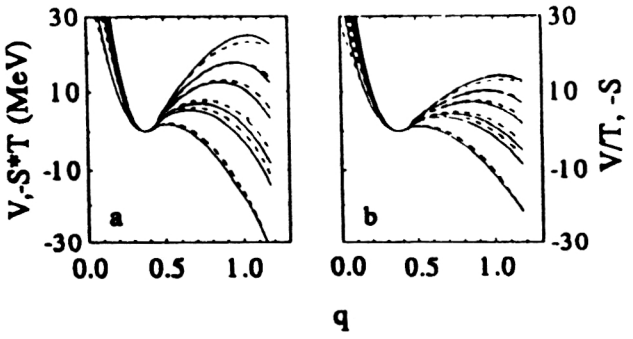

FIG. 5. (a) Potential $V(q)$ (dashed curves) and entropy (with reversed sign) multiplied by the temperature ($-ST$, continuous curves) as functions of the fission coordinate q for ^{178}W (X=0.637), ^{188}Pt (X=0.671), ^{200}Pb (X=0.701), ^{213}Fr (X=0.743), ^{234}Th (X=0.763), and ^{251}Es (X=0.834) (from top to bottom). The calculations were made with the level-density parameter of Ref. 91 for $L=0$ and $E^*_{\rm tot}$ = 50 MeV (Ref. 63). (b) The potential divided by the temperature, $V(q)/T$ (dashed curves), and the entropy (with reversed sign) $-S$ (continuous curves) as functions of the fission coordinate q for the same systems (Ref. 63).

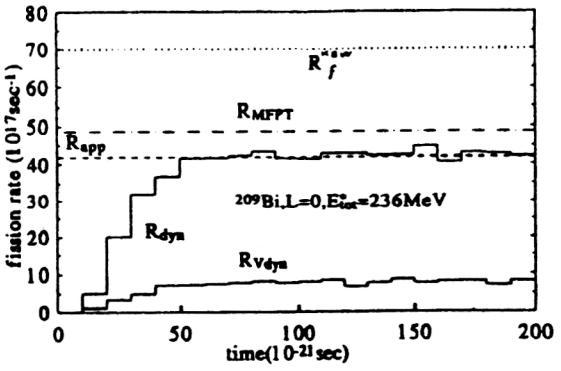

FIG. 6. Fission rates calculated by means of the traditional expressions [$R_{V_{\rm dyn}}$: RLE (12); $R_{\rm f}^{\rm KBW}$: Eq. (22)] and comparison with the results of the modified approach [$R_{\rm dyn}$: RLE (29); $R_{\rm MFPT}$: Eq. (31); and $R_{\rm app}$: Eq. (32)]. The calculations were made with the level-density parameter of Ref. 91 for $E^*_{\rm tot}$ = 50 MeV (Ref. 78).

also shifted to more compact configurations. The reason for both effects is the coordinate dependence of the level-density parameter.

It is interesting to trace the behaviors of the potential energies and, especially, the entropies as functions of the deformation for nuclei with different fissility parameters. The details of this behavior can be clearly seen in Fig. 5. Figure 5a shows V and $-ST$, and Fig. 5b shows $-S$ and V/T. Both the potential and the entropy are normalized to zero in the ground state. The calculations were made for a relatively low excitation energy $\approx$50 MeV and zero angular momentum. For all representations of the results, we see a transition from light systems with high barrier and saddle point lying close to the fission point to heavy systems with low barrier and long descent. These features, which are well known for the potential energy, also persist for the entropy (taken with the opposite sign and appropriately normalized). For the qualitative understanding of the results of the CDSM in the language of entropy, it must be identified with the potential divided by the temperature. For example, $-S_{\rm sd}$=2 means that the fission barrier (in mega-electron-volts) is approximately twice as large as the temperature, and the use of the statistical approach is justified. In contrast, $-S_{\rm sd}$=0.2 means that the fission barrier is five times smaller than the temperature, and to avoid order-of-magnitude errors it is necessary to approach the problem dynamically. A discussion of the details of the mutual relationship of $-S$ and V/T can be found in Ref. 63.

Figure 6 compares the dynamical and statistical descriptions of the fission rates. Here and until the end of this section, $\beta=15\cdot10^{21}$ s^{-1}, corresponding to overdamping. As was to be expected, the dynamical fission rate $R_{V\ \rm dyn}$, calculated in the traditional manner using Eq. (12), does not agree with the statistical fission width $R_{\rm f}^{\rm KBW}$ [expression (22)], which was widely used earlier (Refs. 22, 23, 26, 66, and 72). Whereas $R_{V\ \rm dyn}$ underestimates the true fission rate $R_{\rm MFPT}$, ignoring the surface effects in the level-density parameter, $R_{\rm f}^{\rm KBW}$, in contrast, overestimates the influence of these effects, since it includes the ratio $a_{\rm f}/a_n$, where the value of $a_{\rm f}$ is taken at the saddle point of the *potential energy*, which is deformed much more than the saddle point of the *entropy*. The upshot is that $R_{\rm f}^{\rm KBW}$ exceeds $R_{V\ \rm dyn}$ by more than an order of magnitude.

In our consistent approach, the value of $R_{\rm dyn}$, calculated from the solution of Eq. (29), is close to the modified statistical expression for $R_{\rm MFPT}$ [expression (31)]. In each specific example, the approximate expression for the statistical fission rate $R_{\rm app}$ [expression (32)] even agrees with the dynamical result exactly, but this, of course, is fortuitous.

The dynamical and statistical descriptions of the process are compared in Fig. 7 for the distribution with respect to the deformations of the particles that have not yet reached the scission point. Of course, the picture changes in time until a quasistationary flux through the barrier is established. Figure 7 shows the "relaxed" situation, corresponding to the time $2\cdot10^{-19}$ s. Distributions of the particles corresponding to the canonical [$\exp(-V(q)/T)$] and microcanonical [$\exp(S(q)$] ensembles are compared. It can be seen that the second dis-

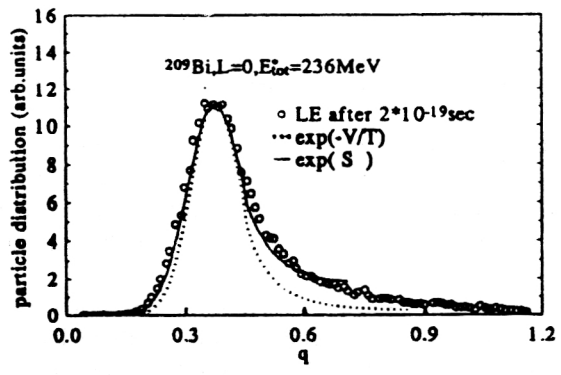

FIG. 7. Distribution of particles that arise in the LFDD with the use of the RLE (29) up to the time $2\cdot10^{-19}$ s (○) and equilibrium distributions obtained using the potential (dotted curve) and entropy (continuous curve). The values of all three distributions are taken to be the same as the maximum.[78]

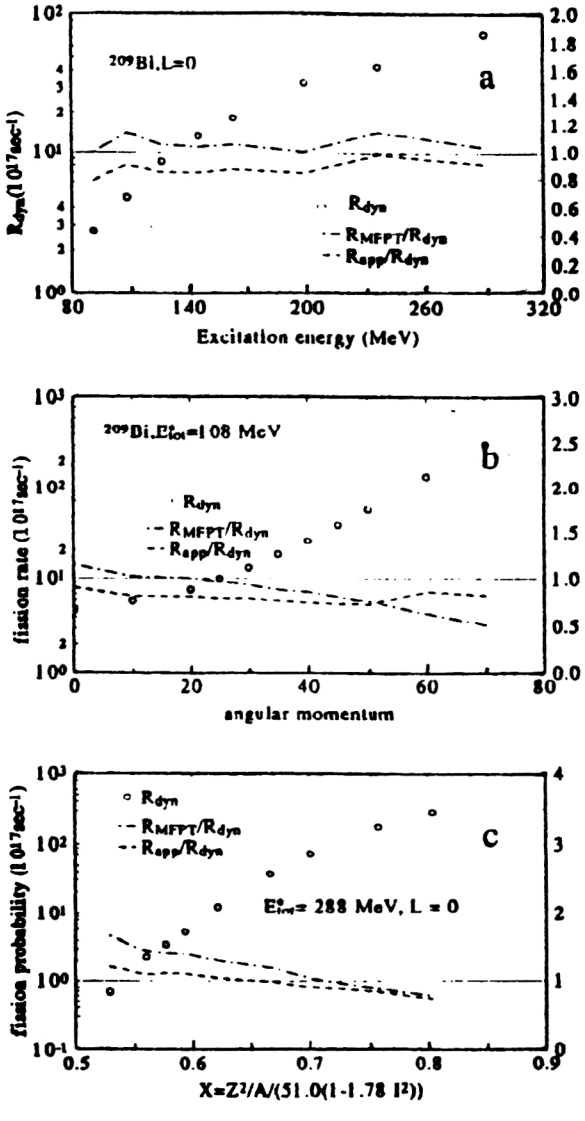

FIG. 8. Quasistationary fission rate obtained dynamically, R_{dyn} (○, left-hand axis), the ratio R_{MFPT}/R_{dyn} (dot–dash curves), and R_{app}/R_{dyn} (dashed curves) calculated (a) for ^{200}Bi at $L=0$ as a function of the internal excitation energy, (b) for ^{209}Bi at E^*_{tot} = 108 MeV as a function of the angular momentum, and (c) for $L=0$ and E^*_{tot} = 288 MeV as a function of the fissility parameter.[78]

tribution agrees much better with the dynamical distribution than the first.

We now turn to a discussion of the consistency of the dynamical [(21) and (29)] and statistical [the "exact" (31) and approximate (32)] fission rates for different excitation energies, angular momenta, and values of the fissility parameter.

Figure 8a shows the dependence of the quasistationary value of R_{dyn} on the excitation energy for the ^{209}Bi nucleus at zero angular momentum. Note that the absolute value of R_{dyn} ranges over almost two orders of magnitude. For the comparison of R_{dyn} with the statistical fission rate, we show the ratios R_{MFPT}/R_{dyn} and R_{app}/R_{dyn}. As can be seen from the figure, the deviations of these ratios from unity do not exceed 20%. The deviations of R_{MFPT} and R_{app} from each other are also about the same. It can be seen that the exact agreement of R_{app} with R_{dyn} in Fig. 6 is indeed fortuitous. A similar test of the consistency of the dynamical and statistical branches of the CDSM for different values of the angular momenta is made in Fig. 8b for the example of ^{290}Bi at $E^*=108$ MeV. Only for very high angular momenta do we observe a discrepancy between the dynamics and statistics greater than 25%. In the practical calculations for such large angular momenta, transition to the statistical branch is not used, since the nuclei fission rapidly in the dynamical regime. In Fig. 8c, we compare the various methods of calculating the fission rates in a wide range of the fissility parameter of the compound nucleus at zero angular momentum and $E^*=288$ MeV. For small values of X, R_{MFPT} and R_{app} exceed R_{dyn}, but with increasing fissility parameter this tendency is replaced by the opposite one. The deviations of R_{MFPT} and R_{app} from R_{dyn} for not too small X again do not exceed 25%. As we have already noted, for light nuclei ($X\leq 0.55$) at zero angular momentum our model ceases to be valid. The increasing deviations of R_{MFPT}/R_{dyn} and R_{app}/R_{dyn} from unity in the region of heavy nuclei are unimportant, since in practical calculations for such nuclei the transition to the statistical branch is not used.

2.6. Distribution of the compound nuclei with respect to the spins[63,72,74]

The distribution of the compound nuclei with respect to the spins has a strong influence of the values of the observable quantities. For this purpose, we used in Refs. 63, 72, 73, and 100 the surface-friction model developed by Fröbrich and collaborators (Refs. 56, 101, and 102) to describe fusion and deep inelastic collisions of heavy ions (it should not be confused with surface one-body dissipation!). This model is based on the one-body mechanism of dissipation proposed by Gross and collaborators (Ref. 8) and on Langevin equations for the collective variables, the role of which is played by the intercenter distance and the deformation of the colliding nuclei. After the calculations, the partial fusion cross sections were approximated by

$$\sigma(l)=\frac{2\pi}{k^2}\frac{2l+1}{1+\exp\left(\frac{l-l_c}{\delta l}\right)}, \tag{45}$$

which was used in the CDSM as a weight function with respect to the partial waves in the dynamical and statistical calculations. A typical dependence of the parameters l_c and δl on the energy of the incident ion for the example of the $^{16}O+^{208}Pb\rightarrow^{224}Th$ reaction is shown in Fig. 9a. The behavior of the diffusivity parameter δl as a function of the energy can be understood on the basis of the simple expression for the mean-square displacement of a free Brownian particle: $\langle y^2\rangle\sim T\cdot t$. At high energies, the temperature becomes higher, the amplitude of the fluctuations is increased, and the diffusivity parameter increases. At low energies, the relative motion of the fusing nuclei becomes slow, and the weak (because of the low temperature) fluctuations have sufficient time to deflect the system significantly from the average path in the phase space. As a result, the diffusivity again increases

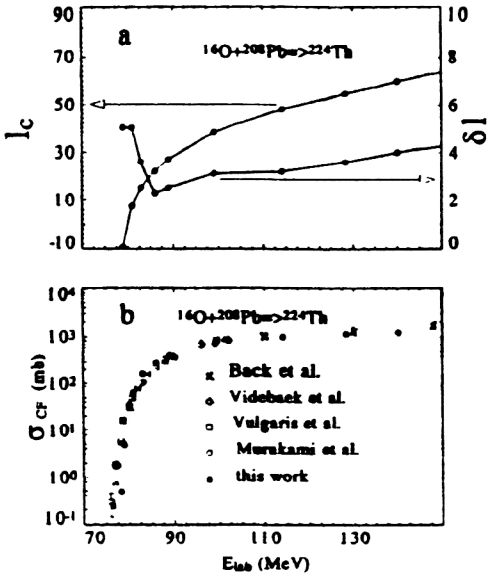

FIG. 9. (a) Parameters of the distribution of the compound nuclei with respect to the spin l_c and δl extracted from calculations in the surface-friction model[56,101,102] for $^{16}O+^{208}Pb$ as a function of the laboratory energy. (b) Experimental fission cross sections for $^{16}O+^{208}Pb\rightarrow^{224}Th$ from Ref. 108 (×), Ref. 109 (◇), Ref. 110 (□), and Ref. 111 (○), compared with the results of calculations in the surface-friction model (Refs. 56, 101, and 102, ●).[73]

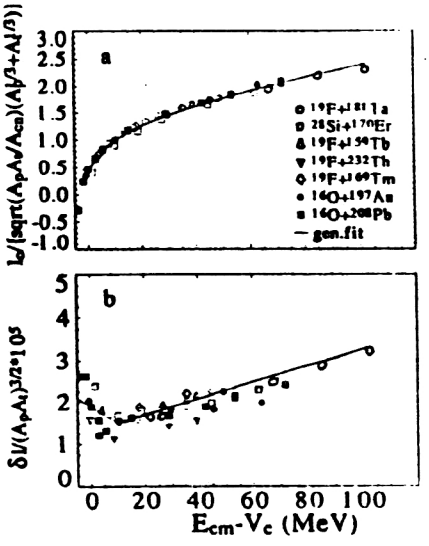

FIG. 10. Results of calculation of the parameters l_c and δl of the distribution of the compound nuclei with respect to the spin by means of the surface-friction model (Refs. 56, 101, and 102), compared with the calculation in accordance with the approximating expressions (46)–(49).[74]

with decreasing energy, but now for a different reason from the case of high energies. The minimum value of δl is attained at intermediate energies of the projectile.

For the example of the $^{16}O+^{208}Pb\rightarrow^{224}Th$ reaction, Fig. 9b shows the quality of the agreement of the fusion cross sections calculated in the surface-friction model[56,101] with the experimental cross sections. This quality is typical for the reactions discussed in the following two sections.

Later, a parametrization of the l_c and δl obtained in the surface-friction model was proposed.[74] For l_c, the parametrization has the form

$$l_c=0.22\cdot\sqrt{(A_p\cdot A_t/A_{cn})}\cdot(A_p^{1/3}+A_t^{1/3})\times(1.5+0.93\sqrt{(E_{cm}-V_c)}),\quad(46)$$

if the energy of the projectile in the center-of-mass system, E_{cm}, is greater than the height of the fusion barrier V_c, for which the simple Coulomb ansatz

$$V_c=5/3\cdot a_c\cdot Z_pZ_t/(A_p^{1/3}+A_t^{1/3}+1.6)\quad(47)$$

with $a_c=0.7053$ MeV is used. For $E_{cm}-V_c>120$ MeV,

$$l_c=2.5\sqrt{(A_p\cdot A_t/A_{cn})}\cdot(A_p^{1/3}+A_t^{1/3}).\quad(48)$$

It is more difficult to parametrize the diffuseness of the distribution of the compound nuclei with respect to the spins. For this purpose, we proposed the ansatz

$$\delta l=\begin{cases}(A_p\,A_t)^{3/2}\cdot10^{-5}\cdot(3+0.04E) & \text{for } E>0,\\ (A_p\,A_t)^{3/2}\cdot10^{-5}\cdot(3-0.08E) & \text{for } E<0.\end{cases}\quad(49)$$

Here $E=E_{cm}-V_c-10$ MeV. Figure 10 illustrates the quality of our parametrization. It is far from perfect, but it is helpful to bear in mind the following. The deviations of the curve constructed in accordance with the expressions (49) from the "exact" values (which, in their turn, are extracted from the results of the calculation in the surface-friction model) play no role in the below-barrier region, since the parametrization was designed from the very beginning to obtain rapidly the distributions of the compound nuclei with respect to the spins when $E_{cm}>V_c$. Exact values of δl are important mainly for light compound systems by virtue of their low fissility, and the most serious inconsistencies between the parametrization and the exact δl arise for comparatively heavy systems ($^{16}O+^{197}Au$, $^{19}F+^{232}Th$), which nevertheless fission with almost 100% probability.

2.7. Algorithm for calculations in the CDSM

The calculations in the CDSM are made in accordance with the following algorithm, which is illustrated in Fig. 11.

The Langevin dynamical calculations begin from the ground state with total excitation energy E^*_{tot} and angular

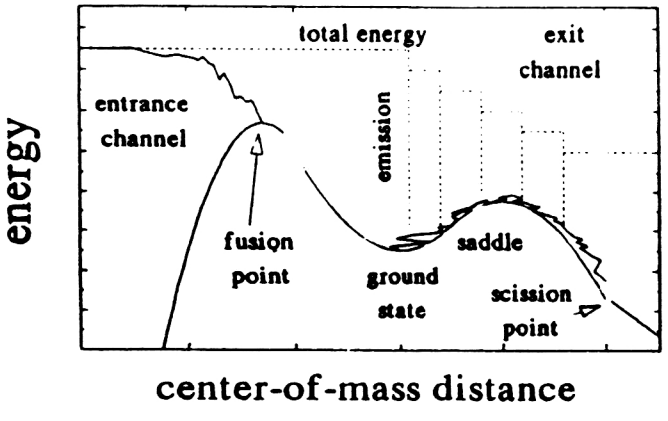

FIG. 11. Qualitative illustration of the logic of calculations in the CDSM.[74]

momentum l. The number of trajectories with given initial conditions is proportional to the partial fusion cross section calculated in accordance with the surface-friction model or in accordance with the parametrization from the previous subsection. Expressed in discrete form, the RLE is

$$q_{n+1}=q_n+\frac{T}{\eta}\left(\frac{dS}{dq}\right)_n\theta+\sqrt{T\theta/\eta}b'(t). \tag{50}$$

Here $b'(t)$ is a normally distributed random variable with variance 2. The emission of light particles and γ rays in the dynamical branch is modeled as follows.[72] For each step in the time θ, the decay widths Γ_ν (ν=n, p, α, d, γ) are calculated. At the same time, we use the expressions for the cross sections of the inverse reactions for the particles[103] that best approximate the exact calculations with optical potentials and the expression for the width for emission of a giant dipole γ ray.[104,105] Then the random number ξ, which is randomly distributed over the interval (0,1), is sampled and compared with the ratio of the integration step of the RLE to the mean emission time τ_{part} ($0\leqslant\xi\leqslant1$; $\tau_{\text{part}}=\hbar\Gamma_{\text{tot}}=\Sigma_\nu\Gamma_\nu$). If $\xi<\theta/\tau_{\text{part}}$, then an emission event is assumed to have taken place, and the species of the emitted particle is established by the usual Monte Carlo scheme in accordance with the partial decay widths, $\Gamma_\nu/\Gamma_{\text{tot}}$. This procedure reproduces, in particular, the radioactive-decay law and is a numerical realization of its differential form. The energy of the emitted particle is calculated by Neumann's method. The integrand in the expression for Γ_ν plays the role of the generating function. After each emission event, the excitation energy, potential, and temperature are recalculated, and the dynamical calculations are continued. The loss of angular momentum is taken into account in a rough approximation: It is assumed that on the average a neutron carries away $1\hbar$, a proton $1\hbar$, an α particle $2\hbar$, a deuteron $2\hbar$, and a γ ray $1\hbar$. These values correspond to the upper bounds of the result obtained in the standard statistical model by the method of Hauser and Feshbach.[71,106]

Ultimately, the dynamical trajectory either reaches the scission point (in this case, a fission event is "detected"), or the internal energy of the particle, which has still not yet reached the saddle point ($q<q_{\text{sd}}$), is reduced to a value

$$E^*<\min(B_\nu,B_{\text{f}}), \tag{51}$$

where B_ν is the binding energy of the particle of species ν, and B_{f} is the fission barrier. The event is then detected as an evaporation remnant.

If neither the one thing nor the other occurs during a certain preassigned time $t=t_{\text{d}}$ and the difference between the entropy in the ground state and at the saddle point exceeds a certain preassigned value S_{STAT},

$$S(q_{\text{gs}})-S(q_{\text{sd}})>S_{\text{STAT}}, \tag{52}$$

then a transition to the statistical branch of the model is made. If the relation (52) does not hold, the dynamical calculations are continued.

Figure 12 shows the multiplicities of prescission neutrons as functions of the parameters t_{d} and S_{STAT} calculated in the CDSM for ^{200}Pb at E^*_{tot} = 150 MeV. It can be seen that $\langle n_{\text{pre}}\rangle$ and the two components of this multiplicity—the part

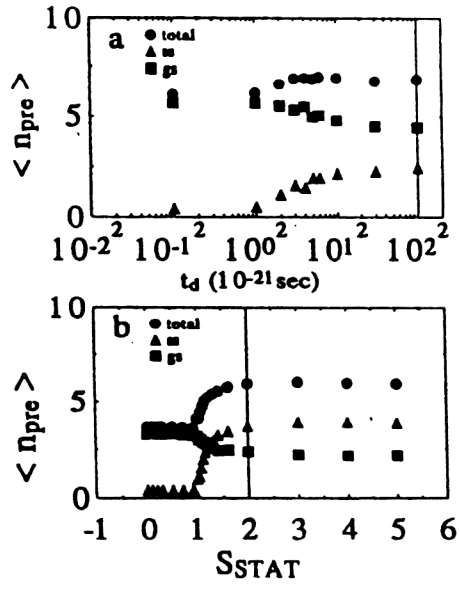

FIG. 12. Results of calculation of the multiplicity of prescission neutrons (●) for ^{200}Pb at total excitation energy 150 MeV as a function of: a) the time t_{d} during which the Langevin calculations are made; b) the parameter S_{STAT}. The contributions of the prefission (gs) and descent (ss) neutrons to $\langle n_{\text{pre}}\rangle$ are also shown. All functions exhibit saturation at $t_{\text{d}}>30\cdot10^{-21}$ s and $S_{\text{STAT}}>1.5$. The calculations were made for $L=50$ and $S_{\text{STAT}}=2$ in case (a) and for $L=60$ and $t_{\text{d}}=0$ in case (b).[63]

emitted before the barrier, $\langle n_{\text{gs}}\rangle$, and the neutrons evaporated during the descent, $\langle n_{\text{ss}}\rangle$—cease to depend on the particular values of t_{d} for $t_{\text{d}}>30\cdot10^{-21}$ s (Fig. 12a). The value of S_{STAT} ceases to affect $\langle n_{\text{pre}}\rangle$ and the components of this multiplicity when $S_{\text{STAT}}>1.5$ (Fig. 12b). The actual values of the parameters t_{d} and S_{STAT} that were used in the calculations, $t_{\text{d}}=100\cdot10^{-21}$ s and $S_{\text{STAT}}=2$, guarantee, thus, that the physical results do not depend on the parameters of the "switching" to the statistical branch.

After the transition to the statistical branch, the partial widths Γ_ν for the emission of particles are calculated in the same way as in the dynamical branch, while the fission width $\Gamma_{\text{f}}=\hbar R_{\text{app}}$ is calculated in terms of the modified fission rate (32). The usual Monte Carlo procedure is used to generate "multichance" fission and subsequent emission of particles. After each emission event, the excitation energy and angular momentum are recalculated, and the calculations are continued until fission occurs or the excitation energy becomes sufficiently small for the condition (52) to hold. Then the event is detected as an evaporation remnant.

3. ANALYSIS OF FISSION CROSS SECTIONS AND THE MULTIPLICITIES OF PRESCISSION NEUTRONS[63,74,75]

3.1. The role of the consistency of the dynamical and statistical descriptions of the fission rate for the analysis of experimental data

In the first subsection of the previous section, we discussed the need for a consistent description of the dynamical and quasistationary stages of the fission process from a gen-

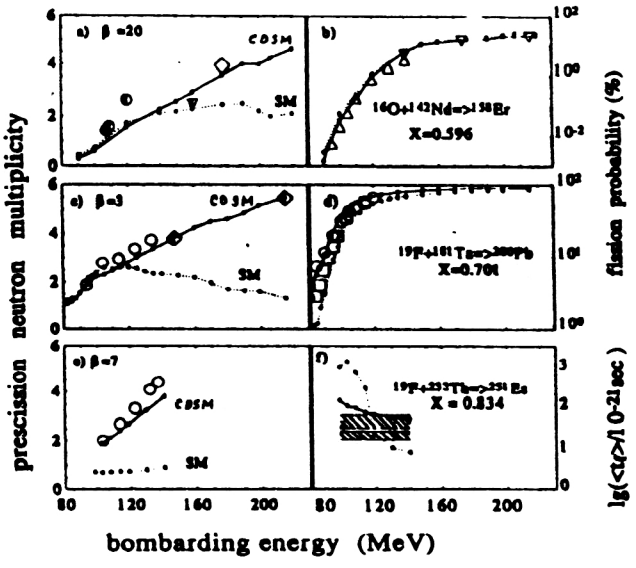

FIG. 13. Multiplicities of prescission neutrons $\langle n_{pre}\rangle$ and fission probabilities P_f for $^{16}O+^{142}Nd\rightarrow^{158}Er$, $^{19}F+^{181}Ta\rightarrow^{200}Pb$, and $^{19}F+^{232}Th\rightarrow^{251}Es$ ($P_f=100\%$) calculated using the Langevin equation (12) and the modified Bohr–Wheeler expression (22) (points joined by solid lines), compared with experimental data. Agreement can be achieved only by using different values of β: ^{158}Er ($\beta=20\cdot10^{21}$ s^{-1}), ^{251}Es ($\beta=7\cdot10^{21}$ s^{-1}), ^{200}Pb ($\beta=3\cdot10^{21}$ s^{-1}). The symbols that show the experimental data for $\langle n_{pre}\rangle$ are: ○ and half-filled circles for $^{18}O+^{150}Sm$ (Ref. 112); ◇ and half-filled diamonds for $^{20}Ne+^{181}Ta$ (Ref. 62); half-filled triangles for $^{18}O+^{144}Sm$ (Ref. 114). The symbols that show P_f and $\langle t_f\rangle$ are: ○ (Ref. 115); □ (Ref. 116); △ (Ref. 117); ▽ (Ref. 118); the hatched region is from Ref. 62 (Ref. 63).

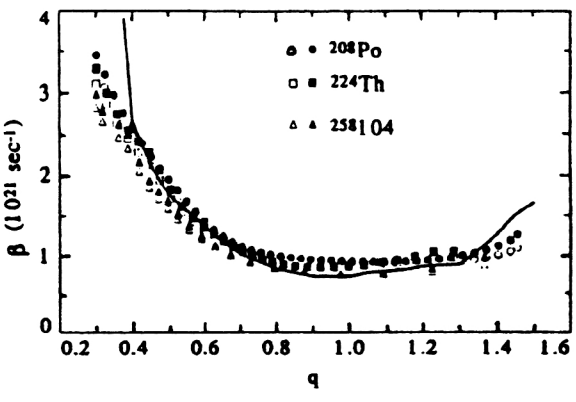

FIG. 14. The damping coefficient β calculated by the Werner–Wheeler method[9] in the model of two-body viscosity as a function of q for three different nuclei.[121] The open symbols are for $\beta=\eta_{qq}/m_{qq}$, and the black symbols for $\beta=\eta_{qq}(m^{-1})_{qq}$. The curve is the calculation of Ref. 119 for ^{213}At, which we have reduced to $\nu_0=2\cdot10^{-23}$ MeV·s·F^{-3} (Ref. 63).

eral theoretical point of view. Here we show that analysis of experimental data also forces us to the modification described in the previous section.

In Ref. 72, the multiplicities $\langle n_{pre}\rangle$ of prescission neutrons and the fission probabilities P_f were calculated for the $^{19}F+^{181}Ta\rightarrow^{200}Pb$ reaction. It was found that the corresponding calculated excitation functions agreed with the experiments for $\beta=3\cdot10^{21}$ s^{-1}. The Sierk barriers[107] and level-density parameter $a(q)$ of Toke and Swiatecki[69] were used. Equation (12) was used to describe the dynamics of the process, and the statistical fission rate was calculated in accordance with (22). In the same approach, it is possible to reproduce the excitation function $\langle n_{pre}\rangle$ and P_f for the $^{16}O+^{142}Nd\rightarrow^{158}Er$ and $^{19}F+^{232}Th\rightarrow^{251}Es$ reactions but with different values of the damping coefficient: $\beta=20\cdot10^{21}$ s^{-1} and $\beta=7\cdot10^{21}$ s^{-1}, respectively.[63] The results of these calculations are illustrated by Fig. 13. Such a situation cannot be recognized as satisfactory, since we are convinced that a physically sensible damping coefficient must be a universal parameter for different systems. This conviction is confirmed by the example shown in Fig. 14. It shows that the damping coefficient calculated by the Werner–Wheeler method[9] for two-body viscosity along the fission valley for nuclei in a wide range of Z and A behaves as a universal function of the fission coordinate q.

Thus, the traditional approach based on Eqs. (12) and (22) is unsatisfactory not only for purely theoretical reasons. It does not enable us to extract a *universal* parameter β from analysis of the experimental data.

3.2. Choice of numerical values for the coefficients of the deformation dependence of the level-density parameter

The situation is changed when we use the CDSM based on Eqs. (29) and (32) and the entropy as a central quantity. Figure 15 shows the results of calculations of the excitation functions $\langle n_{pre}\rangle$ and P_f for seven reactions with three different values of β in a comparison with experimental data. The calculations were made using the Toke–Swiatecki level-density parameter.[69] The experimental excitation functions $\langle n_{pre}\rangle$ are reproduced satisfactorily with the strong damping $\beta=20\cdot10^{21}$ s^{-1} for almost all reactions. The excitation function P_f can be reduced for all reactions with the much less strong damping $\beta=3\cdot10^{21}$ s^{-1}. However, it is still not yet possible to reproduce the multiplicity of the neutrons and the fission probability with the same β. This is not a universal description.

Besides β, there are two "parameters" in the problem that can be varied. These are the set of liquid-drop coefficients in the potential energy [see the expressions (34) and (35)] and the set of coefficients (43) in the expression (42) for $a(q)$.

The set of liquid-drop coefficients influences the height of the fission barrier, the importance of which decreases with increasing energy, as can be seen from the expression (44) for the entropy in the Fermi-gas model. However, our problems are concentrated in the region of high energies; for energies near the Coulomb barrier, the different β give approximately the same $\langle n_{pre}\rangle$. At the same time, the importance of the coordinate dependence of the level-density parameter increases with increasing energy. Therefore, in what follows our attention will be concentrated on it.

To reproduce the experimental data on $\langle n_{pre}\rangle$ and P_f simultaneously with the same damping coefficient, it is necessary to weaken the coordinate dependence $a(q)$ compared with the dependence obtained in Ref. 69. This will make it possible to "close" the fission channel at high excitation energies and to emit more neutrons without changing

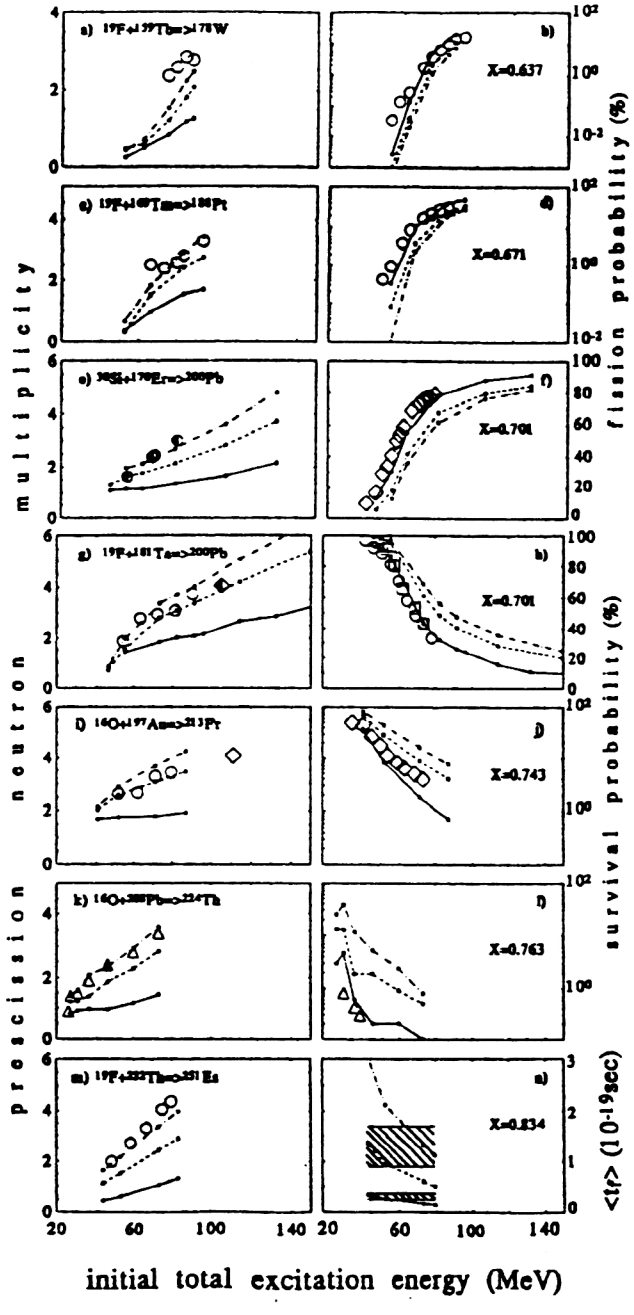

FIG. 15. The values of $\langle n_{pre}\rangle$ and P_f (or the survival probability $1-P_f$) calculated in the CDSM with the level-density parameter of Ref. 69 and a comparison with experimental data. The symbols for $\langle n_{pre}\rangle$: ○ and half-filled circles for $^{28}Si+^{170}Er$ (Ref. 112); ◇ and half-filled diamonds for $^{20}Ne+^{181}Ta$ (Ref. 62); △ (Ref. 120). The symbols for P_f, $1-P_f$, and $\langle t_f\rangle$: ○ (Ref. 115); ◇ (Ref. 25); □ (Ref. 116); △ (Ref. 110); the hatched region is from Ref. 62. The data that are the same as in Fig. 13 are identified by the same symbols. Systematic agreement with the data on $\langle n_{pre}\rangle$ for all systems can be achieved with $\beta=20\cdot10^{21}$ s^{-1} (dot–dash line), whereas for P_f and $1-P_f$ it is achieved with $\beta=3\cdot10^{21}$ s^{-1} (solid lines). The results of the calculations with $\beta=10\cdot10^{21}$ s^{-1} are shown by the broken lines.[63]

strongly the total fission probability, especially at not too large angular momenta.

The existing sets of parameters $\tilde{a}_1$ and $\tilde{a}_2$ in the literature were analyzed by Smirenkin and collaborators in Ref. 87. It follows from this analysis that the Toke–Swiatecki parameters[69] lead to almost the strongest coordinate dependence of the level-density parameter, whereas the parameters of Ignatyuk and collaborators[91] represent the opposite case.

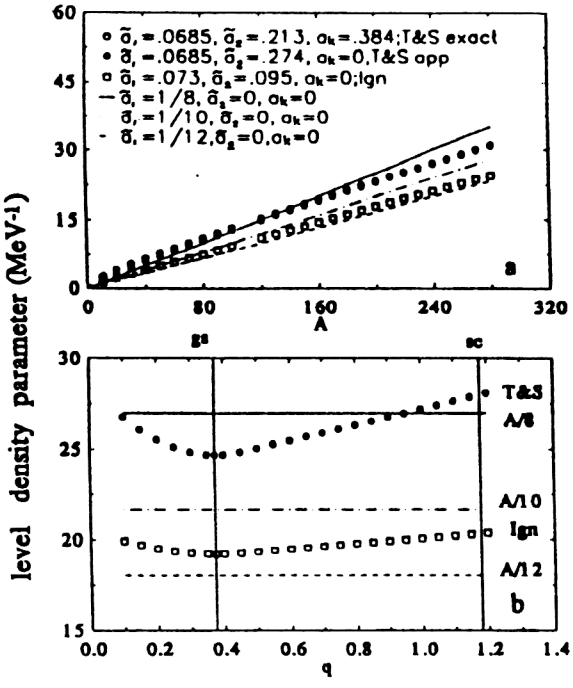

FIG. 16. (a) Liquid-drop level-density parameter of spherical nuclei calculated with different sets of coefficients $\tilde{a}_1$ and $\tilde{a}_2$ in the expression (42) [the term with coefficient a_k responsible for the curvature of the nuclear surface is omitted in the expression (42); for the details, see Refs. 69 and 91] as a function of the mass number: T&S (Ref. 69), Ign (Ref. 91), solid line A/8, dot–dash line A/10, broken line A/12. (b) Coordinate dependence $a(q)$.[63]

The absolute value of the level-density parameter in the ground state obtained by different authors is shown in Fig. 16a as a function of the mass number. The coordinate dependence $a(q)$ is shown in Fig. 16b for $A=216$. Using the weaker coordinate dependence $a(q)$ from Ref. 91, we obtain a satisfactory description of both $\langle n_{pre}\rangle$ and P_f for light and medium nuclei ($X<0.8$) with damping coefficient $\beta=2\cdot10^{21}$ s^{-1}, which corresponds to two-body viscosity $\nu_0=2\cdot10^{-23}$ MeV·s·F^{-3}. The results of the corresponding calculations are shown in Figs. 17a and 17b. However, there is still a certain underestimation of $\langle n_{pre}\rangle$ for ^{200}Pb ($X=0.834$), and this discrepancy increases with increasing energy of the projectile. For heavy systems such as ^{251}Es ($X=0.834$) in Fig. 17c, the calculated multiplicity of the prescission neutrons is much smaller than the experimental multiplicity. The reason for this resides in the two main differences between light and heavy nuclei. The former have a high fission barrier, and a descent section is practically absent; the latter have a low barrier and long descent. Therefore, in the case of ^{200}Pb a large proportion of the neutrons is evaporated when the nucleus (the Brownian particle) fluctuates near the ground state (at least, for not too large laboratory energies), attempting to overcome the higher barrier (*prefission* neutrons). For ^{251}Es, however, a large fraction of all the prescission neutrons must be identified with neutrons evaporated on the descent from the saddle to scission (*descent* neutrons).

Thus, the comparative analysis of $\langle n_{pre}\rangle$ and P_f for light

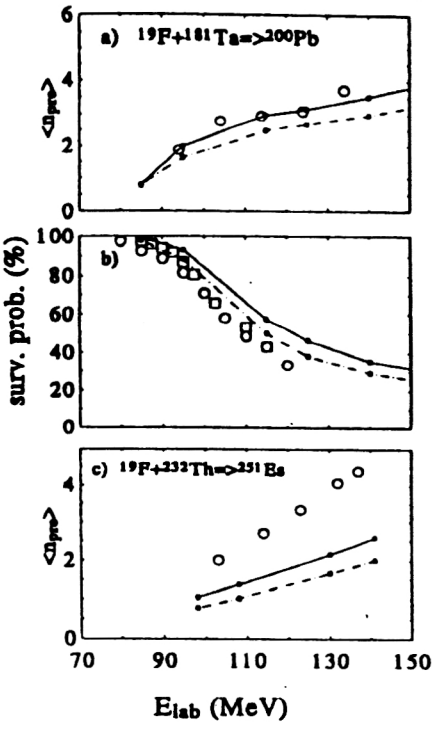

FIG. 17. (a) Multiplicities of prescission neutrons and (b) survival probabilities for ^{200}Pb calculated with the level-density parameter of Ref. 91 and $\beta=2\cdot10^{21}$ s^{-1} (dot–dash lines) and $3\cdot10^{21}$ s^{-1} (solid lines). (c) $\langle n_{pre}\rangle$ for ^{251}Es ($P_f=100\%$) calculated with the same values of the parameters. The experimental data are identified as in Fig. 3 (Ref. 63).

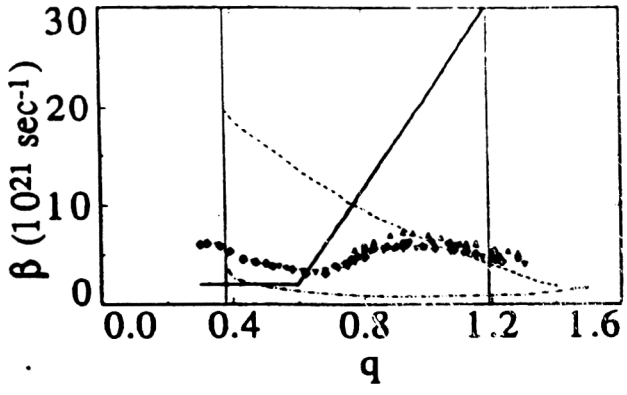

FIG. 18. Damping coefficient β as a function of q. The solid line is the approximation proposed in Ref. 63; the dot–dash curve is the calculation by the Werner–Wheeler method for ^{213}At in the model of two-body viscosity[118] reduced to our $\nu_0=2\cdot10^{-23}$ MeV·s·F^{-3}; the dashed curve is the calculation of Ref. 118 for ^{213}At in the model of one-body dissipation; the solid symbols represent the calculation in the model of surface one-body viscosity with coefficient of reduction of the wall term equal to 0.27 (Ref. 121). The vertical lines show the ground state ($q=0.375$) and the scission point ($q=1.19$).

and heavy systems shows that the dissipative properties of the nuclei near the ground state and during the descent must be different.

3.3. Choice of the damping coefficient of the collective motion along the fission coordinate

In order to reconcile the results of the calculations of $\langle n_{pre}\rangle$ with the experimental data for heavy systems and, simultaneously, to maintain this agreement for light systems, it was proposed to use a coefficient $\beta>2\cdot10^{21}$ s^{-1} but only in the region of deformations where it no longer influences (or influences to a minimal degree) the fissility. A *universal* (i.e., independent of the system) method of doing this is shown in Fig. 18, which gives the damping coefficient β as a function of the deformation. Near the ground state and as far as $q=0.6$, at which a neck of the nucleus begins to form, we use the constant value $\beta=2\cdot10^{21}$ s^{-1}. For $q>0.6$, β increases linearly and reaches the value $\beta_{sc}=30\cdot10^{21}$ s^{-1} at the scission point ($q=1.19$).

This value of β_{sc} is obtained by fitting the multiplicity of prescission neutrons for the ^{19}F+^{232}Th→^{215}Es reaction at energies $E_{lab}=102$ and 137 MeV of the projectile, and it was taken in what follows as universal for all fissioning systems at all energies.

A systematic comparison with experimental data will be made in the following subsection; for the moment, we attempt to explain qualitatively the increase of the damping coefficient. It appears that the dissipation mechanism begins to change its nature when a neck appears in the nucleus. The thinner the neck and the more strongly the incipient fission fragments are individuated, the more the situation resembles the entrance channel of the fusion–fission reaction, where the surface-friction model[101,102] agrees excellently with experiment. However, an estimate of the damping coefficient of the radial motion in the surface-friction model leads to values even greater than $30\cdot10^{21}$ s^{-1}. On the other hand, the entrance reaction channel corresponds to oblate shapes of the reacting partners, whereas the fission fragments before fission have prolate shape. At the same time, the most popular models of dissipation in fission—two-body viscosity,[9] the "wall and window" model,[113] and the surface one-body mechanism[30]—do not lead to the dependence $\beta(q)$ that is required to reproduce systematically the experimental data on $\langle n_{pre}\rangle$ and P_f. This can be seen in Fig. 18. Our conclusion is that the main dissipation mechanism during the descent of the nucleus from the saddle to scission is at present unknown and that the problem does not reduce to a choice between one-body dissipation and two-body viscosity.

3.4. Multiplicities of prescission neutrons and fission probabilities: comparison with experimental data

In this subsection, we present the results of comparison of the theoretical values of the mean multiplicities of prescission neutrons and the fission probabilities with the experimental data for seven compound systems whose fissilities lie in the interval from $X=0.637$ to $X=0.834$ and whose internal excitation energies range from 20 to 200 MeV. The calculations were made with the level-density parameter from Ref. 91 and with the coordinate-dependent damping coefficient from the previous section. For brevity, we shall refer to this set of parameters as the *standard* parameter set. The quality of the agreement between the CDSM and experiment can be gauged from Fig. 19. It is important to note that in the calculations we did not use a single adjustable parameter with values different for different compound systems. Al-

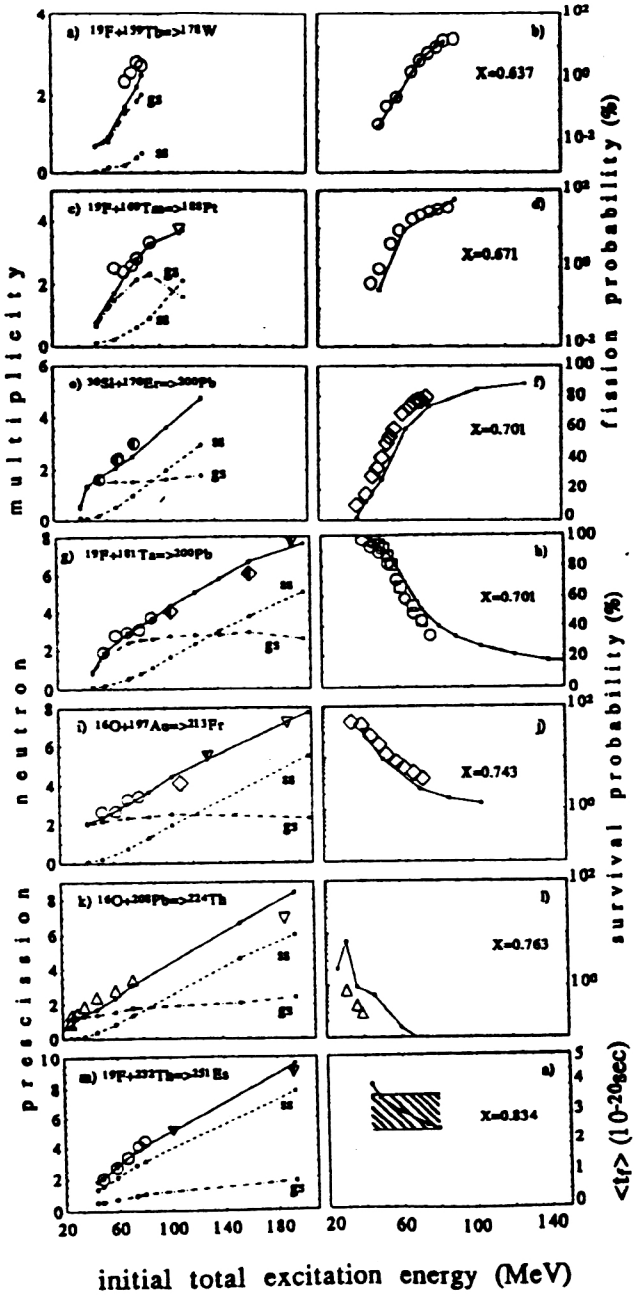

FIG. 19. The values of $\langle n_{pre}\rangle$ and P_f (or the survival probability $1-P_f$) (points connected by the solid continuous lines) calculated in the CDSM with the level-density parameter of Ref. 91 and a damping coefficient that increase sharply on the approach to scission (see Fig. 18) in comparison with experimental data. Figures 19a, 19c, 19e, 19g, 19i, 19k, and 19m also show the prefission (gs) and descent (ss) contributions to $\langle n_{pre}\rangle$. For ^{251}Es (P_f=100%) in Fig. 19n the calculated mean fission times (points connected by the solid continuous lines) are compared with the characteristic fission times extracted from the data on $\langle n_{pre}\rangle$ in Ref. 62 (Fig. 5b) for the similar system Ne+Th (hatched region). The symbols for $\langle n_{pre}\rangle$ are as follows: ○ and half-filled circles for ^{28}Si+^{170}Er (Ref. 112); ◇ and half-filled diamonds for ^{20}Ne+^{181}Ta (Ref. 62); △ (Ref. 120); ▽ and half-filled triangles for ^{18}O+^{169}Tm, c; ^{16}O+^{184}W, g; ^{18}O+^{197}Au, i; ^{18,16}O+^{238}U, m (Ref. 114). The symbols for P_f, $1-P_f$, and $\langle t_f\rangle$ are as follows: ○ (Ref. 115); ◇ (Ref. 25); □ (Ref. 116); △ (Ref. 110); hatched region (Ref. 62). The data that are the same as in Fig. 15 are identified by the same symbols (Ref. 63).

though it does not give perfect agreement with the experiments, our model obviously reproduces the main experimental tendencies in $\langle n_{pre}\rangle$ (see Figs. 19a, 19c, 19e, 19g, 19i, 19k, and 19m) and P_f (Figs. 19b, 19d, and 19f). Instead of the fission probability, Figs. 19h, 19j, and 19l show the survival probability $1-P_f$, for which satisfactory agreement with the experiments is also achieved. The only case in which there is serious disagreement with the data is the survival probability for the ^{16}O+^{208}Pb→^{224}Th reaction (see Fig. 19l). This reaction is discussed in detail in the following section.

Figure 19n shows instead of P_f the mean fission lifetimes, which are obtained naturally in the CDSM. They are in satisfactory agreement with the characteristic, so-called fusion–fission time scales obtained from analysis of experimental data in Ref. 62. The time distributions of fission events will be discussed in more detail in the following section.

We now concentrate our attention on the behavior of $\langle n_{pre}\rangle$ and the two components of it, $\langle n_{gs}\rangle$ and $\langle n_{ss}\rangle$, as the internal excitation energy is changed (Figs. 19a, 19c, 19e, 19g, 19i, 19k, and 19m). In these figures, it can be seen that there are two sections with different slopes of $\langle n_{pre}\rangle$. These slopes are determined by the two different contributions to the prescission multiplicity: the prefission neutrons $\langle n_{gs}\rangle$ and the descent neutrons $\langle n_{ss}\rangle$, which are also shown in the figures. For light systems with a fission barrier greater than or equal to the neutron binding energy and for small projectile energies, the values of $\langle n_{ss}\rangle$ are small compared with $\langle n_{gs}\rangle$, and therefore the low-energy part of $\langle n_{pre}\rangle$ is determined by $\langle n_{gs}\rangle$. For heavy systems and high excitation energies, the $\langle n_{ss}\rangle$ contribution increases. For the systems with the longest descent and the lowest fission barrier, the descent neutrons are predominant at all energies (see Fig. 19m).

The recently published experimental study of Ref. 123 discussed the question of how much of $\langle n_{pre}\rangle$ is evaporated before the saddle and how much during the descent. The conclusions drawn by the authors from the analysis of the distributions of the fragments with respect to the masses and energies qualitatively confirm our theoretical results: For light nuclei at $E^*\approx$50–100 MeV, most of the neutrons are evaporated before the saddle point is passed, whereas for heavy compound systems there must be an appreciable contribution of $\langle n_{ss}\rangle$.

The experimentally found slope $d\langle n_{pre}\rangle/dE^*$ [see Ref. 31, Eq. (3.11)] agrees with the slope of our theoretical curves in the range of energies in which it is determined by the descent neutrons. In this region of energies, the $\langle n_{gs}\rangle(E^*)$ curves reach a plateau. The reasons for this "saturation" and the role of the angular momentum in the energy dependence of $\langle n_{pre}\rangle$, $\langle n_{gs}\rangle$, and $\langle n_{ss}\rangle$ are discussed in detail in Refs. 63 and 64. We mention here that this is a purely heavy-ion effect—it must be absent in reactions induced by light particles.

It is interesting to consider whether the results of the calculations for other observables agree with the experiments and to establish which of these observables are particularly sensitive to the behavior of $\beta(q)$. The following, final section is devoted to this question.

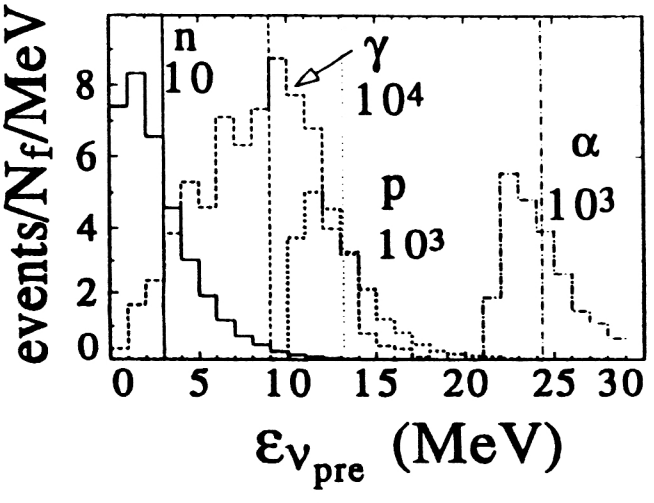

FIG. 20. Spectra of prescission neutrons (n), giant dipole γ rays (γ), protons (p), and α particles (α), normalized to the corresponding mean multiplicities. The calculations were made for $^{16}O+^{208}Pb\rightarrow^{224}Th$ at projectile energy $E_{lab}=140$ MeV. As is indicated in the figure, the spectra are multiplied by 10, 10^4, 10^3, and 10^3 for n, γ, p, and α, respectively. The vertical lines show the mean energies of the corresponding particles (Ref. 73).

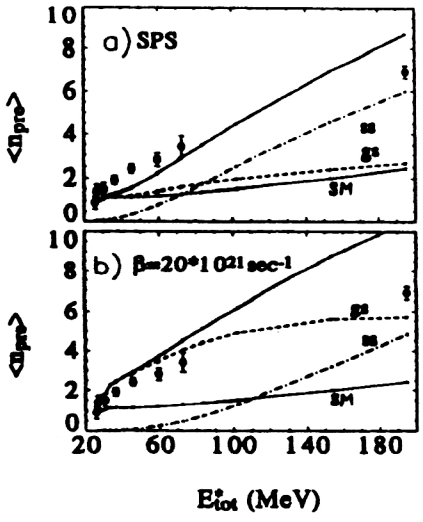

FIG. 21. Results of calculations of the multiplicity $\langle n_{pre}\rangle$ of prescission neutrons for the $^{16}O+^{208}Pb\rightarrow^{224}Th$ reaction in comparison with the experimental data of Refs. 120 and 114 (○) as a function of the excitation energy E^*_{tot}. The calculations in the CDSM were made with (a) the standard parameter set (SPS) and (b) $\beta=20\cdot10^{21}$ s^{-1} (heavy continuous curve). The dot–dash curve shows the contribution of the descent neutrons (ss), and the dashed curve shows the contribution of the prefission neutrons (gs). The thin continuous curve shows the result of the statistical calculation (SM).[73]

4. ANALYSIS OF OTHER OBSERVABLES BY MEANS OF THE CDSM (REFS. 72–76, 100, AND 124–127)

The search for the manifestation of dissipative effects in nuclear fission in other observables besides the energy distributions of the fragments and the mean multiplicities of the prescission neutrons has recently become the subject of many experimental and theoretical studies.[120,128–142]

In particular, the unexpectedly large yield of γ rays in coincidence with fission events found in Refs. 128–131 is interpreted by the authors of those studies as evidence of strong friction with respect to the fission mode in compact configurations. This conclusion contradicts our results presented in the previous section.

To resolve this contradiction, and also to establish which of the observables are most sensitive to the value of the damping coefficient, we made a series of calculations, the results of which are presented in this section. An important difference between these calculations and the ones presented earlier is the greater statistics. Whereas for the analysis of $\langle n_{pre}\rangle$ it is sufficient to calculate several thousand trajectories for one reaction, in this section we present the results of calculations with several hundreds of thousands of trajectories for each reaction. Such a high statistics makes it possible to analyze not only the multiplicity of the neutrons but also that of the charged particles and giant dipole γ rays, and also the spectra of all evaporated particles.

A typical example of such calculated spectra "detected" in coincidence with fission is shown in Fig. 20. The calculations were made with the standard parameter set. The spectra are normalized to the total number of fission events. The calculations were made for the $^{16}O+^{208}Pb$ reaction at laboratory energy 140 MeV. If these spectra are integrated over the energies of the particles, the corresponding prescission multiplicities are obtained. The figure clearly reveals a threshold for emission of protons and α particles that reflects the Coulomb barrier.

4.1. Spectra and multiplicities of prescission neutrons[73]

The influence of the fission dynamics on the spectra and multiplicities of prescission neutrons was investigated theoretically in Refs. 138 and 144. The results of these studies led to the conclusion that the value of the delay time influences the shape of these spectra and that allowance for charged-particle emission leads to an increase in $\langle n_{pre}\rangle$. We made calculations of the spectra of prescission neutrons for the $^{16}O+^{208}Pb\rightarrow^{224}Th$ reaction. This reaction is interesting in that it has been studied by several groups of experimentalists (Refs. 110, 120, 122, and 128–132). Calculations were made not only for the standard parameter set but also for $\beta=20\cdot10^{21}$ s^{-1}, which was extracted in Refs. 128–130 from the spectra of prescission γ rays. This value of β is close to the value obtained in the wall-and-window model for compact configurations (see Fig. 18). This figure also shows the results of calculations in the statistical model made by means of a statistical code that, essentially, is the statistical branch of the program that realizes the CDSM. It differs from the standard statistical codes in using the entropy instead of the potential energy.

In Fig. 21, we compare the results of calculations of $\langle n_{pre}\rangle$ with the experimental data of Refs. 120 and 114 on the multiplicities of prescission neutrons, which are usually regarded as the main indicator of dynamical effects in fission. Figure 21a shows the result of the calculation with the standard parameter set that we have already seen in Fig. 19k and also the purely statistical result. It is obvious that the latter is unsatisfactory. Figure 21b shows the result to which the

CDSM with constant damping coefficient $\beta=20\cdot10^{21}$ s^{-1} leads. As can be seen from the figure, this value also leads to reasonable values of the neutron multiplicities, except for the high-energy point. The two calculations in the CDSM that are compared in Fig. 21 lead to very different $\langle n_{pre}\rangle$ components, which, unfortunately, are not measured in the experiments. These components are also shown in the figures. With the standard parameter set, the prefission multiplicities $\langle n_{gs}\rangle$ are saturated at comparatively low energies, and the observed growth of $\langle n_{pre}\rangle$ is entirely due to the descent neutrons $\langle n_{ss}\rangle$ (Fig. 21a). For $\beta=20\cdot10^{21}$ s^{-1}, the prefission contribution $\langle n_{gs}\rangle$ is predominant up to high energies (Fig. 21b). However, the analysis of the anisotropy of the fragment angular distributions for the considered reaction made by Rossner and collaborators in Ref. 120 shows that for high excitation energies an appreciable number of neutrons are emitted after the saddle point has been passed. This result agrees with the one given in Fig. 21a for the standard parameter set and contradicts the large constant value $\beta=20\cdot10^{21}$ s^{-1} of the damping coefficient. However, this is only an indirect confirmation of the adequacy of our standard parameter set.

Comparing the results of the calculations of the neutron multiplicities, we are forced to the conclusion that by themselves they do not allow us to give preference to one particular coordinate dependence of β over another. However, they do show that the value of β averaged over all deformations has the order of magnitude $(10-20)\cdot10^{21}$ s^{-1}. This value is a few times larger than the value $\beta<4\cdot10^{21}$ s^{-1} obtained in Ref. 144 and the value $\beta<(5-6)\cdot10^{21}$ s^{-1} obtained in Refs. 26 and 36. Thus, the neutron multiplicities carry information about the mean value of the damping coefficient (which is found to be rather large) but are unsuitable for investigating its coordinate dependence.

In accordance with the conclusions of Refs. 138 and 144, independent information about β must be contained in the spectra of the prescission neutrons. These spectra were measured, in particular, by Rossner and collaborators in Ref. 120 for the $^{16}O+^{208}Pb\rightarrow^{224}Th$ reaction. They approximated their results by the Watt spectrum

$$\frac{dN_{n_{pre}}}{d\varepsilon_{n_{pre}}}=\frac{\varepsilon_{n_{pre}}^{1/2}}{\Gamma(3/2)T_{pre}^{3/2}}\exp\left(-\frac{\varepsilon_{n_{pre}}}{T_{pre}}\right). \tag{53}$$

For laboratory energy $E_{lab}=128$ MeV, the parameter T_{pre} was found to be 1.7 ± 0.1 MeV. The corresponding spectrum that we calculated using the standard parameter set is shown in Fig. 22. It agrees well with the experimental spectrum without any special fitting.

In Fig. 23, we compare the measured mean energies of the prescission neutrons as functions of the total excitation energy E^*_{tot} with the results of the CDSM obtained with two coordinate dependences of β (standard parameter set and $\beta=20\cdot10^{21}$ s^{-1}). For comparison, this figure also shows the results of statistical calculations. It can be seen clearly that all three calculations differ very little. Thus, the mean energies of the prescission neutrons *do not* carry information about the dissipative properties of the fission mode.

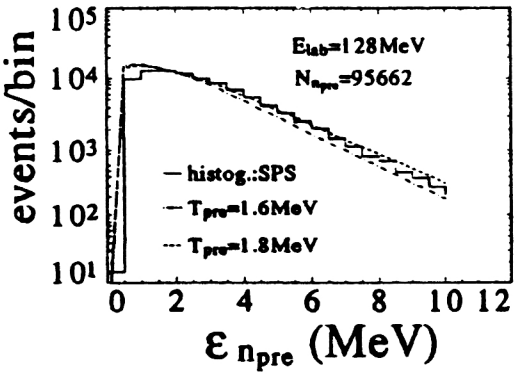

FIG. 22. Spectrum of prescission neutrons (histogram) calculated in the CDSM with the standard parameter set for (128 MeV)$^{16}O+^{208}Pb\rightarrow^{224}Th$ in comparison with the experimental results of Ref. 120, where the spectra were approximated by the Watt spectra with parameter $T_{pre}=1.7\pm0.1$ MeV. The dashed curve and the dot–dash curve correspond to $T_{pre}=1.8$ MeV and $T_{pre}=1.6$ MeV.[73]

4.2. Multiplicities and spectra of charged prescission particles[73,75,76]

We now turn to the charged prescission particles: protons, α particles, and deuterons. Here the experimental situation is rather contradictory. Thus, Ikezoe and collaborators[139] assert that the results of their measurements of the multiplicities of prescission protons, $\langle p_{pre}\rangle$, and α particles, $\langle\alpha_{pre}\rangle$, can be reproduced in the framework of the statistical model without any dissipation ($^{19}F+^{208}Pb$ reaction). On the other hand, Lestone and collaborators[135,136] had to introduce a delay time in order to reproduce the experimental values of $\langle p_{pre}\rangle$ and $\langle\alpha_{pre}\rangle$ in the $^{164,167,170}Er+^{28}Si$ reactions.

In Fig. 24, we compare the prescission multiplicities $\langle p_{pre}\rangle$ and $\langle\alpha_{pre}\rangle$ calculated for the $^{16}O+^{208}Pb$ reaction with the experimental data of Ref. 139 obtained in the similar reaction $^{19}F+^{208}Pb$ (the region of comparatively low energies) and with the data of Ref. 143 obtained in our reaction (point at high energies). The situation is very similar to that

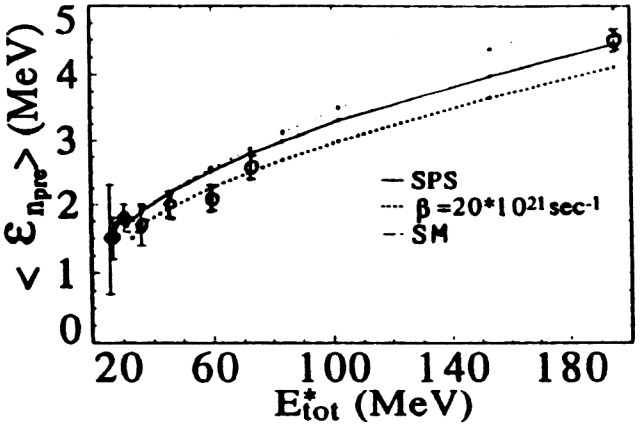

FIG. 23. Mean energies of prescission neutrons calculated for the $^{16}O+^{208}Pb\rightarrow^{224}Th$ reaction as functions of the excitation energy. The calculations were made in the CDSM with the standard parameter set (heavy continuous curve, SPS); with $\beta=20\cdot10^{21}$ s^{-1} (dashed curve); and in the statistical model (thin continuous curve, SM). The experimental data (○) are from Refs. 120 and 114.[73]

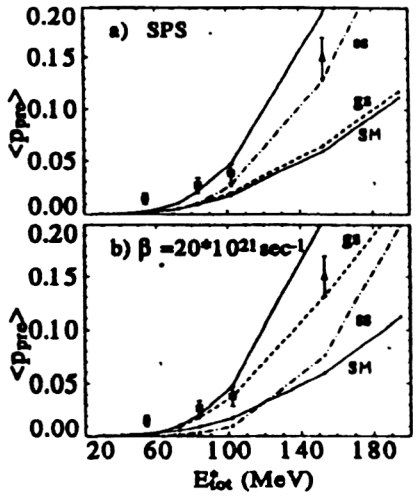

FIG. 24. Mean multiplicities of prescission protons calculated for the $^{16}O+^{208}Pb \rightarrow ^{224}Th$ reaction as functions of the excitation energy. The calculations were made in the CDSM (a) with the standard parameter set (SPS) and (b) with $\beta=20\cdot10^{21}$ s^{-1} (heavy continuous line) and also in the statistical model (thin continuous line, SM). Also shown are the descent (dot–dash lines) and prefission (dashed curve) contributions. The experimental data: □ (Refs. 140 and 141) and △ (Ref. 143).[73]

of the previous subsection for $\langle n_{pre}\rangle$. Our statistical calculation leads to too low values of $\langle p_{pre}\rangle$ and $\langle \alpha_{pre}\rangle$, particularly at high energies, indicating the need to take into account dissipative effects. The values of the multiplicities of prescission protons obtained in the CDSM with the standard parameter set (Fig. 24a) are practically indistinguishable from the values corresponding to $\beta=20\cdot10^{21}$ s^{-1} (Fig. 24b). Only the prefission and descent contributions differ in magnitude, but they are not measured in the experiments. The same can be said of the α particles (see Ref. 73, Fig. 7). The agreement of the calculations with the experiments in Fig. 24 is far from perfect. It can easily be improved, for example, by reducing the Coulomb barrier at low energies (this is a standard fitting device; see, for example, Refs. 136 and 139–141). However, such fitting is not our aim. With regard to high energies, here one expects an enhancement of the preequilibrium emission, leading effectively to a decrease of the excitation energy of the compound nucleus. The experimental points are then shifted toward the theoretical curves.

We also calculated for the $^{16}O+^{208}Pb$ reaction the deuteron prescission multiplicity $\langle d_{pre}\rangle$. At $E_{lab}=215$ MeV, it was found to be 0.037 and 0.034 for the standard parameter set and for $\beta=20\cdot10^{21}$ s^{-1}, respectively. Both values are close to the experimental value 0.030 ± 0.01 of Ref. 143.

The prescission multiplicities of α particles that we calculated with the standard parameter set for the $^{20}Ne+^{197}Au$ reaction are also in satisfactory agreement with the data of Refs. 140 and 141 obtained for the similar $^{19}F+^{197}Ar$ reaction.

Thus, dissipative effects are manifested in the multiplicities of the charged prescission particles only "on the average," and new (compared with $\langle n_{pre}\rangle$) information cannot be extracted.

The situation with regard to the charged-particle spectra appears significantly worse than it does for the multiplicities. In many studies (Refs. 135, 136, 139–141, and 143), it has been noted that the spectra calculated in the framework of the statistical model are shifted to higher energies compared with the experimental spectra. The qualitative explanation of this effect usually reduces to the conclusion that the charged particles are emitted mainly by deformed nuclei, for which the Coulomb barrier is lower than for spherical nuclei. The recent studies of Refs. 135 and 136 discussed one further effect that leads to a softening of the spectrum of charged particles and an enhanced yield of them. This is the decrease in the binding energy of charged particles with increasing deformation of the nucleus. The analysis in Refs. 135 and 136 was made on the basis of the statistical model, and it was assumed that a nucleus emits particles for two fixed deformations, corresponding to the ground state and to the descent from the saddle. This second deformation is an adjustable parameter of the model. The authors were forced to introduce two further adjustable (although universal for the considered systems) parameters: the delay time and the descent time. In Refs. 135 and 136, they used a deformation-dependent level-density parameter a_n in the particle-emission channel but a ratio $a_f/a_n=1$; this is clearly contradictory. Other contradictions are that all the adjustable parameters are independent of the angular momentum and of each other, whereas the delay time and descent time are manifestations of the same dissipative effect. The anomalously large deformation for the nucleus emitting particles during the descent is noteworthy—its value is actually equal to the scission deformation. It cannot be excluded that this is an indication of prompt fission, which one must expect in more symmetric systems and with increasing laboratory energy. It is interesting that much earlier Aleshin[145,146] had already used the mechanism of prompt fission and a deformation-dependent particle binding energy to explain the large values of $\langle p_{pre}\rangle$ and $\langle \alpha_{pre}\rangle$ in reactions leading to comparatively light systems.

To study these dynamical effects in more detail, we calculated the multiplicities and spectra of the charged particles for the $^{28}Si+^{164}Er \rightarrow ^{192}Pb$ reaction, which was studied in Refs. 135 and 136. The results are presented in Fig. 25, in which they are compared with the experimental data of Ref. 136. We see that the CDSM with the standard parameter set (solid curves) reproduces quite well the measured $\langle p_{pre}\rangle$ and $\langle \alpha_{pre}\rangle$ but definitely overestimates the mean kinetic energies of these particles. The same picture is observed for the other reactions. To improve the agreement of the CDSM with experiment for the charged-particle spectra, we took into account, following Ref. 136, the dependence of the particle binding energy and the Coulomb barrier on the deformation. The results of such calculations are shown in Fig. 25 by the dot–dash curve. We find that in a systematic dynamical calculation the influence of these dependences is slight on both the mean multiplicities and the mean energies. The next modification consisted of an additional decrease of the Coulomb barriers in order to bring them into correspondence with the "experimental" values 9.4 MeV for protons and 18.8 MeV for α particles (see Figs. 5 and 6 in Ref. 136). However, this modification too, as can be seen from Fig. 25, does not lead to elimination of the discrepancies with experiment for the mean energies of the prescission α particles. For

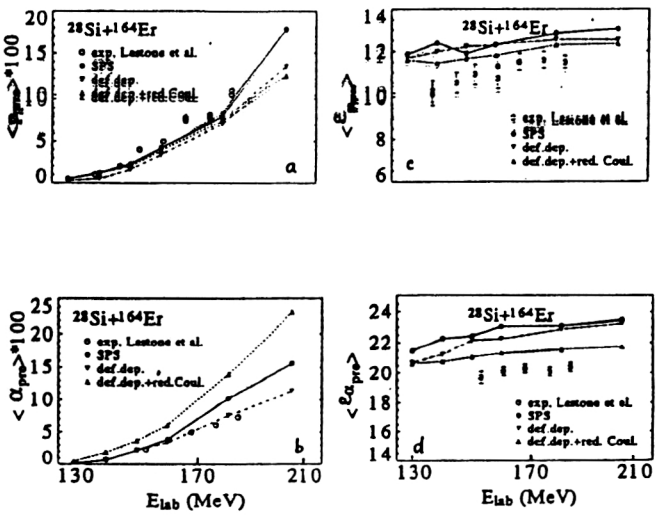

FIG. 25. Mean multiplicities of prescission protons (a) and α particles (b), and also mean energies of prescission protons (c) and α particles (d) calculated for the $^{28}S+^{164}Er\rightarrow^{192}Pb$ reaction as functions of the laboratory energy. The calculations were made in the CDSM with the standard parameter set (●, heavy continuous line), with deformation dependence of the binding energy and the Coulomb barrier (filled inverted triangle, dot–dash line), and with additional reduction of the Coulomb barrier (▲, dashed line). Experimental data: ○ (Ref. 136).

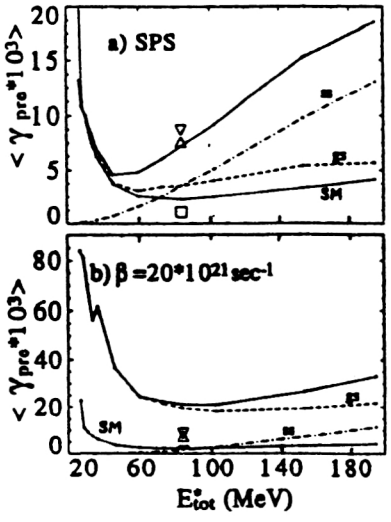

FIG. 26. Mean multiplicities of prescission giant dipole γ rays calculated for the $^{16}O+^{208}Pb\rightarrow^{224}Th$ reaction as functions of the excitation energy. a) The calculations were made in the CDSM with the standard parameter set (heavy solid line) and in the statistical model (thin solid line). Also shown are the descent (dot–dash line) and prefission (broken curve) contributions. b) The same as in (a) but the calculations in the CDSM were made with $\beta=20\cdot10^{21}$ s^{-1}. The figures also show the prescission (▽), descent (□), and prefission (△) γ-ray multiplicities from Ref. 147 (Ref. 73).

the protons, the agreement with experiment for the mean energies becomes much better, but the prescission multiplicities of the α particles now significantly exceed the experimental values.

Thus, the contradiction between the CDSM and experiment for $\langle\varepsilon_{\alpha_{pre}}\rangle$ and $\varepsilon_{p_{pre}}\rangle$ remains uneliminated. However, it is unlikely that we are dealing here with dynamical effects, since there is the same contradiction for the statistical model. It is more likely that there is an effect of the difference between the reaction with absorption of a charged particle by a cold nucleus (this reaction is a source of information about the optical transmission coefficients) and the reaction in which a particle is emitted by a hot rotating nucleus (it is such a reaction with which we are dealing in the decay of the compound system).

4.3. Multiplicities and spectra of prescission γ rays[73,75]

We now discuss the multiplicities of prescission (giant dipole) γ rays $\langle\gamma_{pre}\rangle$ and their spectra. Although there do exist data on the spectra of γ rays in coincidence with fission events,[128–131] we could not extract from the published information *experimental spectra of prescission* γ rays. There is also no direct experimental information about $\langle\gamma_{pre}\rangle$. The corresponding data of the theoretical analysis of Ref. 129 discussed below were communicated to us by D. Hofmann.[147] The aim of our calculations is to confirm the assertion of Ref. 129 that the prescission γ rays are very sensitive to the dynamics of the fission process. In the calculations, we used the standard expression[104] for the rate of decay through the given channel with energy $E_G=80/A^{1/3}$ MeV of the giant dipole resonance and width $\Gamma_G=5$ MeV of the resonance.

As earlier in this section, we compare the results obtained in the CDSM with the standard parameter set and with $\beta=20\cdot10^{21}$ s^{-1}, and also in the statistical approach. The corresponding $\langle\gamma_{pre}\rangle$ are shown in Fig. 26. It can be seen from comparison of Figs. 26a and 26b that the multiplicities calculated with different β differ by a factor in the range 2–7, depending on the excitation energy. The greatest difference is obtained at low excitation energies, where there are no measured data. However, at a total excitation energy around 100 MeV too the prescission γ multiplicities are, as can be seen from the figure, sensitive to the type of friction used in the calculations. For total excitation energy E^*_{tot} = 83 MeV, which corresponds to $E_{lab}=140$ MeV and the energy at which the measurements were made in Ref. 129, the γ multiplicities calculated in the CDSM with different β differ by a factor of about 3 (cf. Figs. 26a and 26b). This difference is much larger than the difference between the corresponding multiplicities of the neutrons and charged particles. Besides our calculations, Fig. 26 also shows the $\langle\gamma_{pre}\rangle$ that we extracted from the calculated spectra of Ref. 147 that best approximate the experimental data at $E_{lab}=140$ MeV (Ref. 129). Against the expectation, these multiplicities agree with ours calculated with the standard parameter set and not with $\beta=20\cdot10^{21}$ s^{-1}, with which the analysis of Refs. 129 and 147 was made. The reason for this unnatural situation is that the authors of Refs. 128–131 do not take into account corrections in the expression for the γ width associated with exchange effects and with the tensor nature of the nuclear forces. As is shown in Ref. 105, these corrections increase the γ width (or the integrated total cross section for photoabsorption) by a factor 1.75 compared with the classical Thomas–Reiche–Kuhn sum rule.[148] After multiplication of the $\langle\gamma_{pre}\rangle$ extracted from Ref. 147 by 1.75, these multiplici-

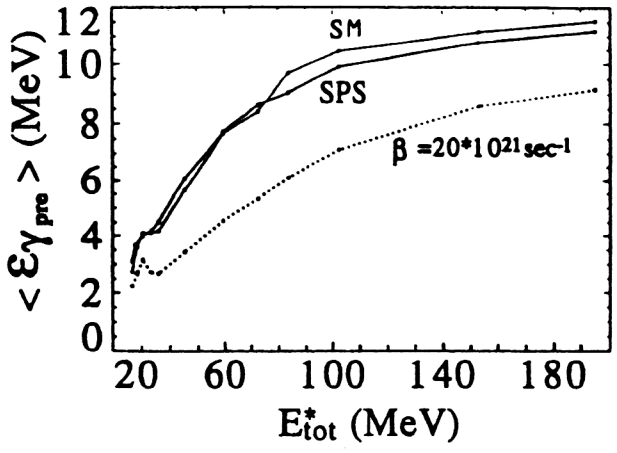

FIG. 27. Mean energies of prescission γ rays calculated for the $^{16}O+^{208}Pb \rightarrow ^{224}Th$ reaction as functions of the excitation energy. Calculations were made in the CDSM with the standard parameter set (heavy solid line, SPS), with $\beta=20\cdot10^{21}$ s^{-1} (broken line), and in the statistical model (thin solid line, SM).[73]

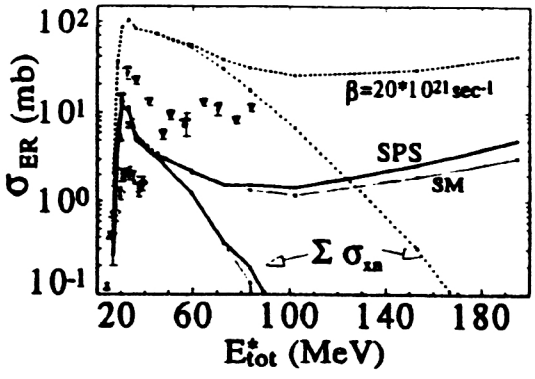

FIG. 28. Cross sections for production of evaporation remnants in the $^{16}O+^{208}Pb \rightarrow ^{224}Th$ reaction as functions of the excitation energy. The thin solid line gives the calculation in the CDSM with the standard parameter set (SPS), the dotted curve gives the calculation in the CDSM with $\beta=20\cdot10^{21}$ s^{-1}, and the thin solid line gives the calculation in the statistical model (SM). The curves to which the arrows point in the lower part of the figure give the contribution of xn reactions. Experimental data: ∇ (Ref. 132), $\triangle$ (Ref. 122), $\diamond$ (Ref. 110).

ties lead, as was to be expected, to satisfactory agreement with our multiplicities calculated with $\beta=20\cdot10^{21}$ s^{-1}.

We now discuss the prefission ($\langle\gamma_{gs}\rangle$) and descent ($\langle\gamma_{ss}\rangle$) contributions to $\langle\gamma_{pre}\rangle$, which are also shown in Fig. 26 for the calculations in the CDSM by the dashed and dot–dash curves, respectively, and for the analysis of Ref. 129 by the open symbols.[147] The prefission contribution is predominant in $\langle\gamma_{pre}\rangle$ from Ref. 147 and in our calculation with $\beta=20\cdot10^{21}$ s^{-1}, as was to be expected. In our dynamical calculations with the standard parameter set, the prefission and descent contributions are approximately equal to each other for the considered total excitation energy E^*_{tot} = 83 MeV. This was to be expected, since friction in the case of the standard parameter set is weak in compact configurations.

Thus, the multiplicities of the prescission γ rays are, judging from everything, very informative as regards the coordinate dependence of the damping coefficient, especially at moderate energies. It would be extremely desirable to obtain direct experimental information about them. We see evidence of strong friction during descent in the enhanced yield of prescission γ rays observed for the spontaneous fission of ^{252}Cf in Ref. 133.

We now turn to a discussion of the spectra of prescission γ rays. The mean energies of the prescission γ rays $\langle\varepsilon_{\gamma_{pre}}\rangle$, calculated in the statistical model and in the CDSM, are shown in Fig. 27. These energies, calculated for $20\cdot10^{21}$ s^{-1}, are much lower than for the standard choice of the parameters or in the statistical model. Thus, in the case of γ rays the mean energies are more sensitive to the coordinate dependence of the damping coefficient than in the case of neutrons and charged particles.

The same features in the behavior of $\langle\gamma_{pre}\rangle$ and $\langle\varepsilon_{\gamma_{pre}}\rangle$ are also found in the calculations that we made for the $^{20}Ne+^{197}Au$ reaction.

Summarizing this subsection, we can say that according to the predictions of the CDSM the prescission dipole γ rays must carry valuable information about the deformation dependence of the damping coefficient. In this respect, their multiplicities, which hitherto have been extracted from the experimental data in a very uncertain manner, are especially informative. Measurement of these multiplicities would be extremely desirable.

The present status of the experimental data on γ rays do not enable us to give preference to one form of friction over another.

4.4. Cross sections for production of evaporation remnants[73–75]

As we already discussed in the previous section, any analysis of experimental data on fusion–fission reactions deserves to be taken seriously only when not only the multiplicities of the prescission particles are reproduced but also the fission probabilities P_f (the fission cross sections divided by the complete-fusion cross section) or the survival probabilities $1-P_f$ (or the corresponding cross sections). Indeed, it was by analyzing the excitation functions n_{pre} and P_f in a wide range of Z and A that in the previous section we obtained the standard parameter set.

For the $^{16}O+^{208}Pb$ reaction, the cross sections for the production of evaporation remnants, σ_{ER}, were measured by Vulgaries and collaborators in Ref. 110 and by Hartel in Ref. 122 for energies near the fusion threshold; the cross sections obtained in Ref. 122 were about three times larger. Recently, we learnt of the study of Brinkmann and collaborators,[132] who measured σ_{ER} from the threshold to laboratory energy 140.5 MeV. These cross sections exceeded by more than a factor 10 at the maximum the results of Vulgaris.[110] All these experimental data are shown in Fig. 28 together with the results of our calculations. The results of the calculations of σ_{ER} with different damping coefficients ($\beta=20\cdot10^{21}$ s^{-1} and the standard parameter set) differ by an order of magnitude, but no conclusions should be drawn, since the spread of the

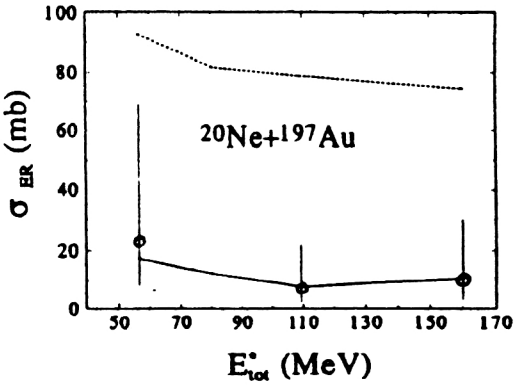

FIG. 29. Cross sections for production of evaporation remnants in the $^{20}Ne+^{197}Au \rightarrow ^{217}Ac$ reaction as functions of the excitation energy. The continuous line gives the calculation of the CDSM with the standard parameter set, and the dotted line gives the calculation in the CDSM with $\beta=20\cdot10^{21}$ s^{-1}. Experimental data: ○ (Ref. 142).[75]

experimental data is too great. It is obvious that the situation must be clarified in the first place by the experimentalists.

Figure 28 shows the contribution of the *xn* reactions to the total σ_{ER}. It can be seen that the high-energy part of the excitation function for production of evaporation remnants owes its existence entirely to reactions with emission of a charged particle (or particles). The growth of σ_{ER} in the region of high laboratory energies is explained by the fact that after the emission of a proton or an α particle the daughter nucleus becomes less fissile and survives with a greater probability. This mechanism works with ever increasing efficiency with increasing excitation energy, since then the importance of the Coulomb barrier decreases. The corresponding growth appears to be revealed in Fig. 28 in the experimental data of Ref. 132. The effect was apparently observed by Hessberger and collaborators[142] for the $^{20}Ne+^{197}Au$ reaction. The corresponding experimental data are shown in Fig. 29, where the results of our calculations in the CDSM are compared with them. It can be seen that the standard parameter set leads to good agreement with the experimental values of σ_{ER}, whereas the calculation with $\beta=20\cdot10^{21}$ s^{-1} overestimates these cross sections by a factor in the range 5–10. It is interesting that Hessberger and his collaborators[142] interpreted the growth of σ_{ER} as a manifestation of dissipative effects. In our calculation with the standard parameter set, everything that occurs up to the saddle point does not differ too much from the results of the standard statistical model; it is during the descent from the saddle to scission that dynamics mainly plays a role. The growth of σ_{ER} at high energies in the CDSM is a purely statistical effect; the numerical value of β determines only the absolute magnitude of σ_{ER} but not the energy dependence of this cross section. Recalling that for this reaction we also have reasonable agreement with the data on the multiplicities of charged particles, we may conclude that the analysis of the $^{20}Ne+^{197}Au$ reaction appears to support the conclusion that the main features of the coordinate dependence of the level-density parameter and the damping coefficient are correctly reproduced in our standard parameter set.

4.5. Time distributions of fission events (Refs. 63, 73, 100, and 124–127)

The most direct information about the dynamics of fission and, in particular, its dissipative properties, is contained in the time distribution $P(t_f)$ of the fission events. However, attempts to extract this information encounter serious obstacles. First, it is rather difficult to measure $P(t_f)$ directly. Second, the influence of the dynamics on $P(t_f)$ may be masked by purely statistical effects.

The first difficulty can be overcome by measuring only a part of the distribution $P(t_f)$ that is of the greatest interest. For example, in Refs. 116 and 149 measurements were made of the lifetimes to fission of compound nuclei from Hg to Fr produced in reactions induced by heavy ions. In these measurements, which were made by the blocking method,[150,151] a so-called *long-lived fission component* was found. It is characterized by a quantity χ_L that, by definition, is the fraction of fission events corresponding to times greater than a certain time t_L; usually, t_L is taken equal to 10^{-16} s (χ_{16}) or $3\cdot10^{-17}$ s (χ_{317}). The particular choice of t_L is due to the details of the blocking method.

The appearance of a long-lived fission component for compound nuclei from Hg to Fr is explained in Ref. 116 by fission events that occur in the final state of an evaporation cascade. In this region of compound nuclei, it was found to be possible to describe the magnitude and energy dependence of χ_{317} (or χ_{16}) by means of a statistical model that takes into account shell and pairing effects.[149]

However, as the calculations of Refs. 124 and 125 showed, macroscopic statistical effects play the decisive role in the appearance of the long-lived fission component. Examples of the results of such calculations are presented in Table I. They show that the macroscopic statistical calcula-

TABLE I. Comparison of the results of calculations of the long-lived fission component in the macroscopic statistical model with experimental data.

Reaction	E_{lab}, MeV	E^*, MeV	χ_{16}^{max},% theor.	χ_{16}^{max},% exp.	Reference
$^{12}C+^{nat}W \rightarrow Hg$	80–87	56–63	12	14	[116]
$^{16}O+^{nat}W \rightarrow Pb$	90–115	50–73	12	22	[116]
$^{19}F+^{181}Ta \rightarrow ^{200}Pb$	90–120	51–78	12	16	[149]
$^{12}C+^{nat}W \rightarrow Bi$	95	52	14	16	[116]
—	108	64	8	10	[116]
$^{16}O+^{197}Au \rightarrow ^{213}Fr$	90	43	6	<10	[116]

TABLE II. Comparison of the results of calculations of the long-lived fission component in the macroscopic statistical model for reactions that have not yet been studied experimentally.

E_{lab}, MeV	E^*, MeV	χ_{16}, (%)	σ_f, (mb)
	$^{12}C+^{209}Bi\rightarrow^{229}Ac$		
55	29.7	5.2	0.103
60	34.4	12.7	20.2
65	39.1	11.1	266
70	43.9	2.5	555
75	48.6	0.4	798
	$^{14}C+^{197}Au\rightarrow^{211}Rn$		
65	39.1	22.0	0.309
70	43.8	27.5	37.5
75	48.4	25.8	231
80	53.1	10.4	457
85	57.8	9.2	693
	$^{16}O+^{181}Ta\rightarrow^{197}Tl$		
80	46.0	0.1	4.56
85	50.6	3.9	20.7
90	55.2	8.4	70.6
95	59.7	9.1	192
100	64.3	11.2	373
110	73.5	8.4	710
	$^{40}Ca+^{135}Ba\rightarrow^{175}Os$		
170	51.4	0.5	0.130
175	55.2	8.1	2.47
180	59.1	15.3	25.9
185	62.9	4.3	95.9

tion agrees satisfactorily with the data of Refs. 116 and 149.

The quantity χ_{16}^{max} given in this table is the maximum value of χ_{16} for the given energy interval. It is interesting to note that in Ref. 152 Bugrov and Karamyan "did not find a large contribution of a long-lived ($\tau > 10^{-16}$ s) component to the total fission cross section" for the $^{16}O+^{nat}W\rightarrow Pb$ reaction (second row in Table I). Thus, from the experimental point of view the situation is not entirely definite.

In Ref. 124, macroscopic statistical calculations of the time distributions of fission events for reactions that have not yet been studied by the blocking method were made. The results of these calculations, which can be regarded as theoretical predictions, are presented in Table II.

For compound nuclei for which the fission barrier at zero angular momentum is above the neutron binding energy, the results of the calculations in the framework of the CDSM with the standard parameter set and with $\beta = 20 \cdot 10^{21}$ s^{-1} give a result for the long-lived fission component close to the statistical result. This is demonstrated in Fig. 30. However, it should be noted that the calculation corresponding to a large constant damping coefficient was made with the level-density parameter of Ref. 69, whereas the standard parameter set includes the level-density parameter of Ref. 91.

Thus, in the region of nuclei for which the fission barrier at zero angular momentum lies above the neutron binding energy the long-lived fission component does not carry information about the dynamics of the fission process. At the same time, this quantity (for reactions with heavy ions) has hitherto been measured by only two groups, the results of which do not agree. According to the calculations of Refs. 124 and 125, the presence of a long-lived component in the

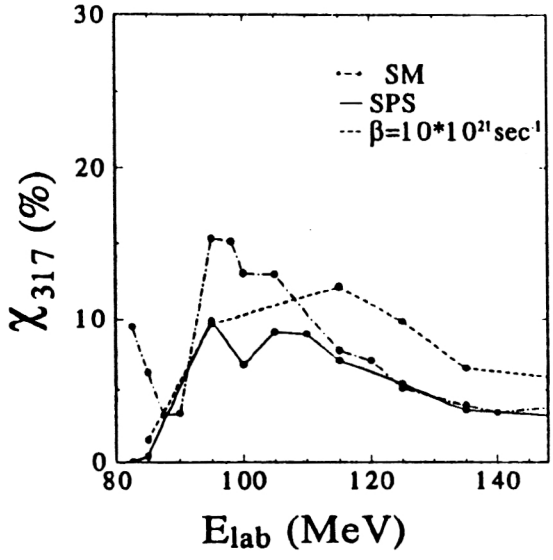

FIG. 30. Long-lived fission component as a function of the laboratory energy for the $^{19}F+^{181}Ta\rightarrow^{200}Pb$ reaction. The dot–dash line gives the calculation in the statistical model (SM), the solid line gives the calculation in the CDSM with the standard parameter set (SPS), and the broken line gives the calculation in the CDSM with $\beta = 20 \cdot 10^{21}$ s^{-1}.

fission of nuclei with $Z^2/A \leqslant 36$ produced in reactions with heavy ions for $\langle l_f \rangle \approx l_{B_f}$ is the rule rather than the exception. Corresponding measurements would be extremely desirable and could be informative with regard to the statistical aspects of the process. Thus, the detailed measurements of the lifetime of actinides under the influence of light particles made by Yuminov and collaborators[153] demonstrated the importance of taking into account the coefficient of rotational enhancement of the level density.

The situation with regard to the extent to which the long-lived fission component gives information about the dynamics will evidently be radically changed on the transition to the heaviest fissioning systems produced in heavy-ion reactions. For excited intermediate systems with $Z^2/A \geqslant 38$, the fission barrier decreases rapidly, and its role could be taken over by nuclear friction if it is not so small, as in our standard parameter set. The existence of a long-lived fission component for such systems would be a direct confirmation of appreciable dissipation in the region of compact nuclear configurations. Therefore, measurements of the long-lived fission component for heavy systems must be very informative about the dynamics of the fission process in general and the dissipative properties of the fission mode in particular. We shall discuss below the results of Ref. 100, which confirm this conclusion.

In addition to the model described in Sec. 2, this work took into account the temperature-dependent shell corrections to the entropy, which, as before, determines the dynamics of the process. The allowance was done by the method proposed by Ignatyuk and collaborators in Ref. 91. The "regeneration" of the shells that accompanies cooling of a nucleus as it emits neutrons must have a decisive effect on the entire fission process of excited actinide nuclei.

Figure 31 shows time distributions of fission events for

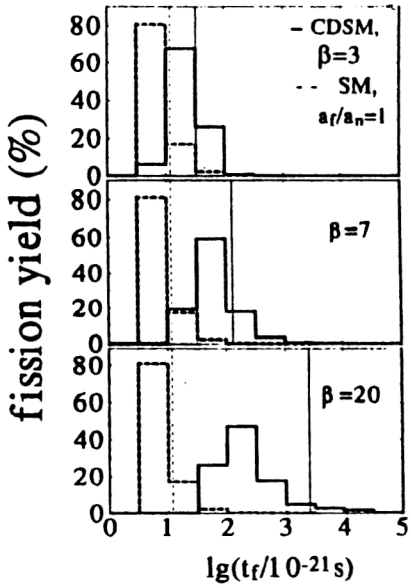

FIG. 31. Distribution of fission events with respect to the time calculated for the (98 MeV)^{19}F+^{232}Th→^{251}Es reaction. The calculations made in the statistical model are represented by the dashed histograms, and those in the CDSM by the solid histograms. The values of β are shown in units of 10^{21} s^{-1}. The vertical lines are the mean values of the corresponding distributions.[100]

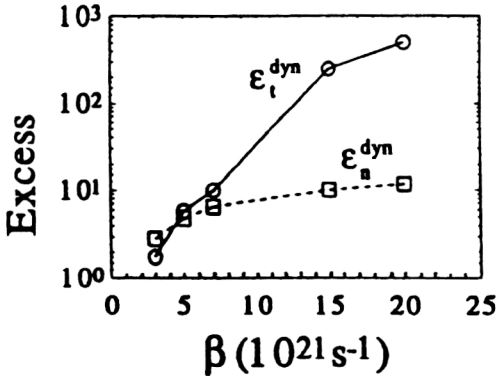

FIG. 32. Excess of statistical values for the mean fission time [see Eq. (55)] and for the multiplicity of prescission neutrons [see Eq. (56)] as functions of β. The calculations were made for the (98 MeV)^{19}F+^{232}Th→^{251}Es reaction.[100]

the ^{19}F+^{232}Th→^{251}Es reaction. We emphasize that in these calculations we used not the standard parameter set but constant (not dependent on the deformation) values of β and $a_f/a_n=1$. It can be seen that the histograms obtained by means of the CDSM differ appreciably from the statistical ones, especially at large values of β. Independently of the method of calculation, the distributions are found to be very broad and asymmetric (the logarithm is plotted along the abscissa!). These distributions are not at all similar to the familiar Gaussian distribution, and therefore the mean fission time $\langle t_f \rangle$, which is shown in Fig. 31 by the vertical lines, does not reflect the lifetime of the majority of events. In other words, $\langle t_f \rangle$ is appreciably greater than the *most probable* fission time t_f^{mp}; sometimes, they do not even agree in order of magnitude. As can be seen from Fig. 31, the mean fission time $\langle t_f \rangle$ reflects if anything the behavior of the long-lived "tail" of the distribution $P_f(t)$. For $\beta \geq 7 \cdot 10^{21}$ s^{-1}, a few percent of the events occur at times greater than 10^{-18} s. According to Refs. 150 and 151, such times can be measured by means of the blocking method. In the reaction that we are discussing (^{19}F+^{232}Th), the reason for the occurrence of the long-lived component is nevertheless "multiple chance" fission. However, the factor that suppresses fission in the first stages of the evaporation cascade is here friction, whereas for ^{19}F+^{181}Ta, for example, the fission competes strongly with neutron emission, where it is found that the condition

$$B_f(l_c) \approx B_n \tag{54}$$

holds.[116] Here $B_f(l)$ is the height of the fission barrier, which depends on the angular momentum, B_n is the neutron binding energy, and l_c is the critical angular momentum for fusion. Thus, for heavy systems the long-lived fission component contains information about nuclear dissipation for compact configurations, and in this sense has advantages over the mean multiplicity of prescission neutrons.

Figure 32 presents the results of calculations of

$$\varepsilon_t^{dyn} = \frac{\langle t_f^{dyn} \rangle - \langle t_f^{SSM} \rangle}{\langle t_f^{SSM} \rangle} \tag{55}$$

and

$$\varepsilon_n^{dyn} = \frac{\langle n_{pre}^{dyn} \rangle - \langle n_{pre}^{SSM} \rangle}{\langle n_{pre}^{SSM} \rangle}, \tag{56}$$

which show qualitatively the extent to which the mean fission time and the mean multiplicity of the prescission neutrons give information about the value of the damping coefficient. As we have seen in this section, at the present time $\langle n_{pre} \rangle$ is the only measured quantity that exhibits systematic deviations from the predictions of the statistical model. Here we demonstrate, following Ref. 100, that χ_L for heavy systems may also be a more sensitive indicator of dynamical effects. First, as can be seen from Fig. 32, for large values of β the quantity ε_t^{dyn} exceeds ε_n^{dyn} by more than an order of magnitude. The rate of growth of ε_t^{dyn} with increasing damping coefficient is also much larger than for ε_n^{dyn}. Recalling that the behavior of $\langle t_f \rangle$ is determined by the long-lived "tail" of the distribution of the fission events with respect to the time, we arrive at the conclusion that the long-lived fission component is not only an indicator of dynamical effects but is even their "enhancer."

Fragmentary experimental information on the existence of χ_{16} or χ_{217} was published by Karamyan and collaborators for the reactions ^{238}U+^{12}C (Ref. 154) and ^{238}U+^{22}Ne (Ref. 155). The existence of χ_{218} and χ_{918} was apparently detected by Molitoris and collaborators[134] in the fission of uranium-like products after deep inelastic collisions of ^{238}U nuclei with each other. The authors of Refs. 154 and 155 assume that χ_L arises in their experiment through fission of weakly excited target-like products of transfer reactions. It would be very important to confirm or refute this explanation by means of additional and more systematic measurements. For this, we proposed[100] the investigation of χ_L in reactions with nonfissioning targets, for example, ^{32}S+^{208}Pb or ^{31}P+^{209}Bi.

TABLE III. Long-lived fission components for the $^{208}Pb+^{32}S$(176 MeV) reaction calculated in the framework of the CDSM and in the statistical model. The liquid-drop and shell parts of the fission barrier are B_f^{ld} and B_f^{sh}, respectively; χ_{318} is the long-lived fission component for $t_L=3\cdot10^{-18}$ s calculated in the CDSM; $\langle t_f^{CDSM}\rangle$ and $\langle t_f^{SSM}\rangle$ are the mean fission times calculated in the CDSM and in the statistical model, respectively.

A/a_n, MeV	a_f/a_n	B_f^{ld}, MeV	B_f^{sh}, MeV	χ_{318}, %	$\langle t_f^{CDSM}\rangle$ 10^{-18} s	$\langle t_f^{SSM}\rangle$ 10^{-18} s
9.1	1.01	1.8	4.2	4.0	8.3	0.011
—	—	—	5.2	9.8	50.6	0.013
—	—	—	3.2	2.5	1.6	0.009
—	—	2.8	4.2	13.4	54.1	0.406
—	—	0.8	—	0.4	0.3	0.005
—	1.00	1.8	—	4.6	8.8	0.024
—	0.99	—	—	5.7	8.4	0.033
8.0	1.01	—	—	2.7	3.4	0.012
10.0	—	—	—	7.0	4.0	0.011
12.0	—	—	—	8.3	15.6	0.013

In order to make some predictions about the possible results of such experiments, calculations were made in Ref. 100 of the lifetime until fission for the $^{208}Pb+^{32}S$(176 MeV) reaction with $\beta=20\cdot10^{21}$ s^{-1}, this being a value that the authors of the measurements of the spectra of prescission γ rays extract from their data.[129] The results of these calculations, made in the CDSM and the statistical model, are presented in Table III. It can be seen that the existence of χ_{318} for $\beta=20\cdot10^{21}$ s^{-1} is clearly predicted by the CDSM independently of the uncertainties in the parameters of the model. On the other hand, no variation of the parameters of the statistical model can make the mean fission times calculated by means of it similar to the dynamical times.

Thus, systematic and detailed experimental investigation of the phenomenon of the long-lived fission component for reactions that lead to heavy intermediate systems may open up a possibility for a definitive conclusion concerning nuclear friction for compact configurations. Such an investigation would help to resolve the contradiction that arises between different authors in the determination of the damping coefficients.

As we have already mentioned, the mean fission times often differ very strongly from the most probable times. Figure 33 shows the mean fission times $\langle t_f\rangle$ and the most probable fission times t_f^{mp} obtained in the framework of the CDSM with the standard parameter set. The calculation was made for 11 reactions that lead to a compound nucleus with excitation energy 100 MeV. To ensure that the distributions of the compound nuclei with respect to the spin do not depend too strongly on the reaction, the ^{19}F ion was used throughout as the projectile. Figure 33 also shows the characteristic experimental fission times extracted from data on $\langle n_{pre}\rangle$.[114] They agree reasonably with t_f^{mp} in the complete range of Z. In contrast, the mean times approach t_f^{mp} and the experimental times only for heavy compound systems.

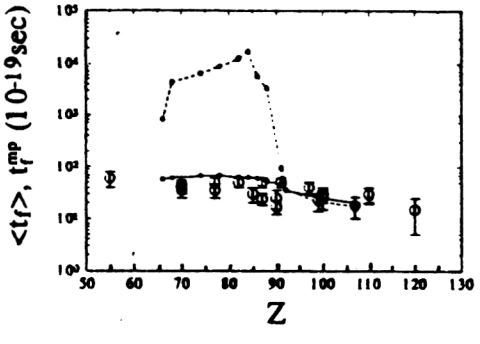

FIG. 33. Mean fission time $\langle t_f\rangle$ (dashed line, ●) and most probable fission time t_f^{mp} (solid line, ●) as functions of the charge number of the compound nucleus. The calculations were made in the CDSM with the standard parameter set. Experimental data: ○ (Ref. 114).

Thus, the mean multiplicity of prescission neutrons and the long-lived fission component are mutually complementary sources of information about nuclear viscosity and the characteristic times of the fission process. Whereas $\langle n_{pre}\rangle$ carries information about the viscosity averaged over all deformations and about the most probable times of the process, the long-lived fission component carries information about friction in compact configurations and about the mean fission time.

4.6. Fragment excitation energy at the scission point[126]

The large prescission neutron multiplicities indicate that the fission process is sufficiently slow for the compound nucleus to lose a significant fraction of its initial excitation energy. Since the neutron emission time $\langle t_n\rangle$ depends strongly on the excitation energy, most systems will evaporate neutrons until $\langle t_n\rangle$ for the last prescission neutron is equal in magnitude to the most probable fission time. As a result of this, the internal excitation energy of most systems at the scission point must be small and should not depend strongly on the initial excitation energy. Hinde and collaborators[156] proved this by analyzing *the mean postscission neutron multiplicities* $\langle n_{post}\rangle$ for a wide range of compound nuclei. In the framework of the CDSM, it is not possible to calculate $\langle n_{post}\rangle$.

However, it is possible to compare the calculated values of the mean internal excitation energies of the system before scission with the values extracted from the data on $\langle n_{post}\rangle$. Such a comparison is shown in Fig. 34 for seven different compound systems. The curves correspond to the calculation in the CDSM with the standard parameter set. The satisfactory agreement with experiment confirms the conclusion that

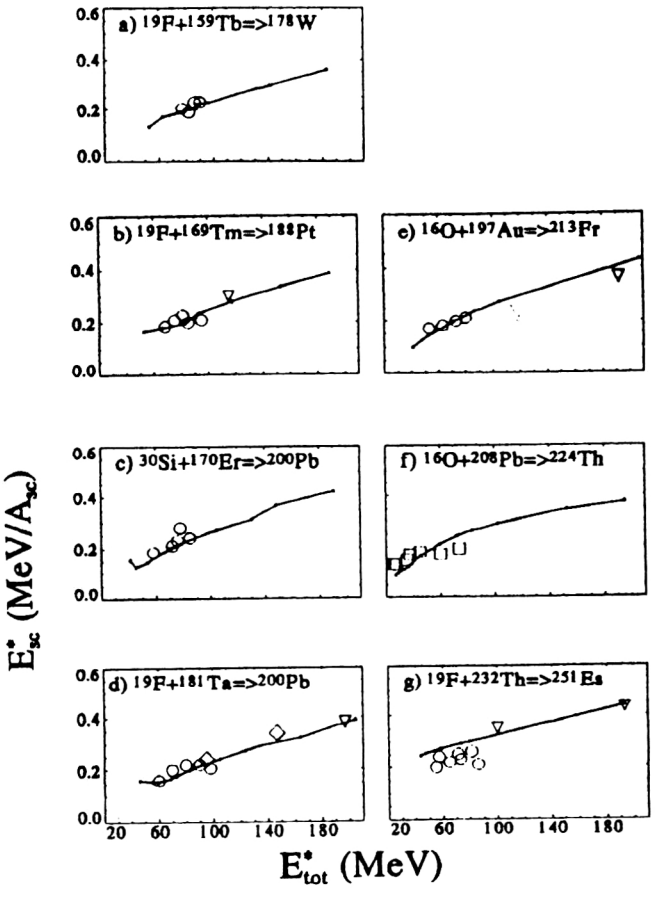

FIG. 34. Excitation energy per nucleon at the scission point as a function of the initial excitation energy for seven compound systems. The calculations were made in the CDSM with the standard parameter set (curves). Experimental data: ○ (Ref. 112), ◇ (Ref. 34), ▽ (Ref. 114), □ (Ref. 120) (Ref. 126).

on the average the damping coefficient is fairly large. However, data of this kind do not carry information about the details of the coordinate dependence of β.

CONCLUSIONS

The main content of this review has been an analysis of experimental data that carry information about the dissipative properties of the fission mode. This analysis has been mainly made by means of the combined dynamical–statistical model, which has been developed during the last four years.

It was shown that it is possible, without using adjustable parameters for individual nuclei, to reproduce the data on the fission cross sections and also on the multiplicities of prescission neutrons and charged particles in a wide range of the fissility parameter and the excitation energy of the compound nuclei obtained in heavy-ion fusion. Agreement with the experiments is achieved by using the so-called standard parameter set: with a comparatively weak deformation dependence of the level-density parameter and with a damping coefficient of the fission mode that depends strongly on the deformation. This coefficient is comparatively small for weakly deformed configurations and increases sharply on the formation of a neck between the incipient fragments, reaching its maximum value at the scission point. None of the models of nuclear viscosity existing in the literature predicts such behavior of the damping coefficient. Thus, the problem arises of creating an adequate model of nuclear dissipation.

The analysis has also shown that all the observable quantities can be divided into three classes.

In the first class, we must put those observables that can be reproduced in the framework of the statistical model. They are the probability (or cross section) of fission and its "conjugate" observable—the survival probability—and also the mean energies of the prescission neutrons and charged particles. By themselves, they do not carry information about the damping coefficient β of the collective motion, but their values impose restrictions on the parameters of the statistical model. Here there has been accumulated a huge volume of experimental data, and the task of the theory is to describe them without the use of unjustified adjustable parameters that take values that cannot be predicted for each new compound system.

In the second class, we put the quantities that contain information, averaged over all deformations, about the dissipative properties of the fission mode. We have here the multiplicities of prescission and postscission particles. The set of data indicates that on the average β is large compared with the predictions of two-body viscosity, which is capable of reproducing the data on the distributions of the fragments with respect to the kinetic energies. Here the amount of experimental material is also great. However, there remain gaps for reactions induced by light particles.

Finally, in the third class we have the observables that apparently contain information about the dependence of the dissipative properties on the shape of the fissioning nucleus. These are the cross sections for production of evaporation remnants and the long-lived fission component for nuclei with a low barrier, and also the mean multiplicities and energies of the prescission γ rays. Here the experimental data are as yet insufficient, and they are often contradictory.

I wish to express my sincere gratitude to Yu. A. Lazerev, V. V. Pashkevich, G. N. Smirenkin, and P. Fröbrich, the collaboration with whom largely determined the content of this review. I am sincerely grateful to my colleagues and coauthors D. Hilscher, H. Rossner, and G. I. Kosenko. I benefited greatly from regular contacts and discussions on various parts of the paper with A. V. Ignatyuk, M. G. Itkis, V. M. Kolomiĭts, and A. Ya. Rusanov, to whom I express my deep thanks.

This review was written with financial support of the International Science Foundation (Grant NRG000).

[1] D. Hilscher, Pramana J. Phys. **33**, 1 (1989).
[2] N. Bohr and J. A. Wheeler, Phys. Rev. **56**, 426 (1939).
[3] H. A. Kramers, Physica (Utrecht) **7**, 284 (1940).
[4] V. M. Strutinsky, Phys. Lett. B **47**, 121 (1973); Yad Fiz. **19**, 259 (1974) [Sov. J. Nucl. Phys. **19**, 127 (1974)].
[5] E. Cheifetz *et al.*, Phys. Rev. C **2**, 256 (1970).
[6] Z. Fraenkel, J. P. Unik, A. J. Gorski, and W. D. Loveland, Phys. Rev. C **12**, 1809 (1975).
[7] V. V. Volkov, *Deep Inelastic Nuclear Transfer Reactions* [in Russian] (Énergoatomizdat, Moscow, 1982).
[8] D. H. E. Gross and H. Kalinowski, Phys. Rep. **45**, 175 (1978).

[9] K. T. R. Davies, A. J. Sierk, and J. R. Nix, Phys. Rev. C **13**, 2385 (1976).
[10] K. T. R. Davies, R. A. Managan, J. R. Nix, and A. J. Sierk, Phys. Rev. C **16**, 1890 (1977).
[11] P. Grange, H. C. Pauli, and H. E. Weidenmüller, Phys. Lett. B **88**, 9 (1979).
[12] P. Grange, H. C. Pauli, and H. A. Weidenmüller, Z. Phys. A **296**, 107 (1980).
[13] G. D. Adeev and I. I. Gonchar, Yad. Fiz. **37**, 1113 (1983) [Sov. J. Nucl. Phys. **37**, 780 (1983)].
[14] G. D. Adeev and I. I. Gonchar, Yad. Fiz. **40**, 869 (1984) [Sov. J. Nucl. Phys. **40**, 553 (1984)].
[15] G. D. Adeev and I. I. Gonchar, Z. Phys. A **320**, 451 (1985).
[16] G. D. Adeev, I. I. Gonchar, L. A. Marchenko, and N. I. Pischasov, Yad. Fiz. **43**, 1137 (1986) [Sov. J. Nucl. Phys. **43**, 727 (1986)].
[17] G. D. Adeev and I. I. Gonchar, Z. Phys. A **322**, 479 (1985).
[18] O. A. Serdyuk *et al.*, Yad. Fiz. **46**, 710 (1987) [Sov. J. Nucl. Phys. **46**, 399 (1987)].
[19] G. D. Adeev, I. I. Gonchar, and L. A. Marchenko, Yad. Fiz. **42**, 42 (1985) [Sov. J. Nucl. Phys. **42**, 25 (1985)].
[20] P. Grange and H. A. Weidenmüller, Phys. Lett. B **96**, 26 (1980).
[21] P. Grange, Li-Jang Qing, and H. A. Weidenmüller, Phys. Rev. C **27**, 2063 (1983).
[22] S. Hassani and P. Grange, Phys. Lett. B **137**, 281 (1984).
[23] S. Hassani and P. Grange, Z. Phys. A **325**, 95 (1986).
[24] W. P. Zank *et al.*, Phys. Rev. C **33**, 519 (1986).
[25] D. J. Hinde *et al.*, Nucl. Phys. A **452**, 550 (1986).
[26] A. Gavron *et al.*, Phys. Rev. C **35**, 579 (1987).
[27] D. J. Hinde *et al.*, Phys. Rev. C **37**, 2923 (1988).
[28] G. Wegmann, Phys. Lett. B **50**, 327 (1974).
[29] J. J. Griffin and M. Dworzecka, Nucl. Phys. A **455**, 61 (1986).
[30] J. R. Nix and A. J. Sierk, Int. School-Seminar on Heavy Ion Physics, Dubna, USSR, September 22–30, 1986, No. D7-87-68, Dubna (1987), p. 453.
[31] D. Hilscher and H. Rossner, Ann. Phys. (Paris) **17**, 471 (1992).
[32] K. Pomorski and H. Hofmann, Phys. Lett. B **263**, 164 (1991).
[33] B. W. Bush, G. F. Bertsch, and B. A. Brown, Phys. Rev. C **45**, 1709 (1992).
[34] Yu. A. Lazarev, At. Energ. Rev. **15**, 75 (1977).
[35] M. G. Itkis, V. N. Okolovich, A. Ya. Rusanov, and G. N. Smirenkin, Fiz. Elem. Chastits At. Yadra **19**, 701 (1988) [Sov. J. Part. Nucl. **19**, 301 (1988)].
[36] S. M. Luk'yanov *et al.*, Int. School-Seminar on Heavy Ion Physics, Dubna, USSR, October 3–12, 1989, No. D7-90-142 [in Russian], Dubna (1990).
[37] S. V. Zhdanov *et al.*, Yad. Fiz. **55**, 3169 (1992) [Sov. J. Nucl. Phys. **55**, 1766 (1992)].
[38] S. V. Zhdanov *et al.*, Yad Fiz. **56**, No. 2, 55 (1993) [Phys. At. Nucl. **56**, 175 (1993)].
[39] F. Scheuter, C. Gregoire, H. Hofmann, and J. R. Nix, Phys. Lett. B **149**, 303 (1984).
[40] G.-R. Tillack, Phys. Lett. B **278**, 403 (1992).
[41] J. R. Nix, Nucl. Phys. A **130**, 241 (1969).
[42] T. Wada, Y. Abe, and N. Carjan, Phys. Rev. Lett. **70**, 3538 (1993).
[43] G.-R. Tillack *et al.*, Phys. Lett. B **296**, 296 (1992).
[44] G. D. Adeev *et al.*, Fiz. Elem. Chastits At. Yadra **19**, 1229 (1988) [Sov. J. Part. Nucl. **19**, 529 (1988)].
[45] D. Cha and G. F. Bertsch, Phys. Rev. C **46**, 306 (1992).
[46] P. Grange *et al.*, Phys. Rev. C **34**, 209 (1986).
[47] E. Strumberger, K. Dietrich, and K. Pomorski, Nucl. Phys. A **529**, 522 (1991).
[48] R. L. Stratonovich, *Topics in the Theory of Random Noise* (Gordon and Breach, New York, 1963), Vols. 1 and 2.
[49] N. G. van Kampen, *Stochastic Processes in Physics and Chemistry* (North-Holland, Amsterdam, 1981).
[50] S. Chandrasekhar, *Stochastic Problems in Physics and Astronomy* (AIP, New York, 1943) [Russ. transl., IL, Moscow, 1947].
[51] Y. Abe, C. Gregoire, and H. Delagrange, J. Phys. (Paris) **47**, No. C-4, 329 (1986).
[52] P. Fröbrich and S. Y. Xu, Nucl. Phys. A **477**, 143 (1988).
[53] P. Fröbrich and J. Stroth, Phys. Rev. Lett. **64**, 629 (1990).
[54] P. Fröbrich and J. Richert, Phys. Lett. B **237**, 328 (1990).
[55] P. Fröbrich, *Dissipation and Thermal Fluctuations in Heavy-Ion Collisions* (Springer-Verlag, Berlin, 1991), p. 93.
[56] J. Marten and P. Fröbrich, Nucl. Phys. A **545**, 854 (1992).
[57] H. Hofmann, A. S. Jensen, and F. J. Scheuter, *Proc. of the 12th Int. Symposium on Nuclear Physics*, Report NISSN 0138-2950, Gaussig, GDR (1982), p. 96.
[58] S. Ayik, E. Suraud, J. Stryewski, and M. Belkacem, Z. Phys. A **337**, 413 (1990).
[59] D. Boilley, E. Suraud, Y. Abe, and S. Ayik, Nucl. Phys. A **556**, 67 (1993).
[60] R. Stokstad, in *Treatise on Heavy Ion Science*, edited by D. A. Bromley (Plenum Press, New York, 1985), Vol. 3, p. 82.
[61] Yu. Ts. Oganessian and Yu. A. Lazarev, in *Treatise on Heavy Ion Science*, edited by D. A. Bromley (Plenum Press, New York, 1985), Vol. 4, p. 3.
[62] D. J. Hinde *et al.*, Phys. Rev. C **39**, 2268 (1989).
[63] P. Fröbrich, I. I. Gontchar, and N. D. Mavlitov, Nucl. Phys. A **556**, 281 (1993).
[64] I. I. Gonchar and H. D. Mavlitov, Yad. Fiz. **53**, 1567 (1991) [Sov. J. Nucl. Phys. **53**, 963 (1991)].
[65] H. A. Weidenmüller, Nucl. Phys. A **471**, 1c (1987).
[66] P. Grange, Nucl. Phys. A **428**, 37c (1984).
[67] G. D. Adeev, I. I. Gonchar, V. V. Pashkevich, and O. A. Serdyuk, Yad. Fiz. **50**, 1242 (1989) [Sov. J. Nucl. Phys. **50**, 774 (1989)].
[68] J. O. Newton, Fiz. Elem. Chastits At. Yadra **21**, 821 (1990) [Sov. J. Part. Nucl. **21**, 349 (1990)].
[69] J. Toke and W. J. Swiatecki, Nucl. Phys. A **372**, 141 (1981).
[70] E. G. Lanza and H. A. Weidenmüller, Z. Phys. A **323**, 157 (1986).
[71] H. Delgrange, C. Gregoire, F. Scheuter, and Y. Abe, Z. Phys. A **323**, 437 (1986).
[72] N. D. Mavlitov, P. Fröbrich, and I. I. Gontchar, Z. Phys. A **342**, 195 (1992).
[73] P. Fröbrich and I. I. Gontchar, Nucl. Phys. A **563**, 326 (1993).
[74] P. Fröbrich and I. I. Gontchar, Second Int. Conf. on Dynamical Aspects of Nuclear Fission, June 14–18, 1993, Smolenice, Slovakia, E7-94-19, JINR, Dubna (1994), p. 182.
[75] I. I. Gontchar and P. Fröbrich, Yad. Fiz. **57**, 1249 (1994) [Phys. At. Nucl. **57**, 1181 (1994)].
[76] I. I. Gontchar and P. Fröbrich, Second Int. Conf. on Dynamical Aspects of Nuclear Fission, June 14–18, 1993, Smolenice, Slovakia,, E7-94-19, JINR, Dubna (1994), p. 182.
[77] I. I. Gontchar and P. Fröbrich, Nucl. Phys. A **551**, 495 (1993).
[78] I. I. Gontchar, P. Fröbrich, and N. I. Pischasov, Phys. Rev. C **47**, 2228 (1993).
[79] I. I. Gonchar and G. I. Kosenko, Yad. Fiz. **53**, 133 (1991) [Sov. J. Nucl. Phys. **53**, 86 (1991)].
[80] G. I. Kosenko, I. I. Gonchar, O. I. Serdyuk, and N. I. Pischasov, Yad. Fiz. **55**, 920 (1992) [Sov. J. Nucl. Phys. **55**, 514 (1992)].
[81] I. I. Gonchar, G. I. Kosenko, and N. D. Mavlitov, *Proceedings of the International Conference "Fifty Years of Fission,"* October 16–20, 1989, Leningrad, USSR [in Russian], V. G. Khlopin Radium Institute, St. Petersburg (1992), p. 295.
[82] P. Fröbrich and G.-R. Tillack, Nucl. Phys. A **540**, 353 (1992).
[83] H. J. Krappe, *Proc. of the Int. Workshop on Dynamical Aspects of Nuclear Fission*, Smolenice, June 17–21, 1991, CSFR. E7-92-95, JINR, Dubna (1992), p. 51.
[84] T. Wada, N. Carjan, and Y. Abe, Nucl. Phys. A **538**, 283 (1992).
[85] A. V. Ignatyuk *et al.*, Yad. Fiz. **40**, 625 (1984) [Sov. J. Nucl. Phys. **40**, 400 (1984)].
[86] A. V. Ignatyuk *et al.*, Yad. Fiz. **40**, 1404 (1984) [Sov. J. Nucl. Phys. **40**, 892 (1984)].
[87] E. M. Rastopchin, Yu. B. Ostapenko, M. I. Svirin, and G. N. Smirenkin, Yad. Fiz. **49**, 24 (1989) [Sov. J. Nucl. Phys. **49**, 15 (1989)].
[88] A. Bohr and B. R. Mottelson, Nuclear Structure, Vol. 2 (Benjamin, London, 1975), p. 371.
[89] H. Hofmann, Phys. Lett. B **61**, 423 (1976).
[90] H. Hofmann, R. Samhammer, and G. Ockenfuss, Nucl. Phys. A **496**, 269 (1989).
[91] A. V. Ignatyuk *et al.*, Yad. Fiz. **21**, 1185 (1975) [Sov. J. Nucl. Phys. **21**, 612 (1975)].
[92] R. Balian and C. Bloch, Ann. Phys. (N.Y.) **60**, 401 (1970).
[93] L. D. Landau and E. M. Lifshitz, *Statistical Physics*, Parts 1 and 2, 3rd ed. (Pergamon Press, Oxford, 1980) [Russ. original, Parts 1 and 2, 3rd ed., Nauka, Moscow, 1976].
[94] P. Hänggi, P. Talkner, and M. Borcovec, Rev. Mod. Phys. **62**, 251 (1990).
[95] L. A. Pontryagin, A. Andronov, and A. Vitt, Zh. Éksp. Teor. Fiz. **3**, 165 (1933).
[96] W. D. Myers and W. J. Swiatecki, Nucl. Phys. **81**, 1 (1966); Ark. Fys. **36**, 343 (1967).

[97] M. Brack *et al.*, Rev. Mod. Phys. **44**, 320 (1972).
[98] R. W. Hasse and W. D. Myers, *Geometrical Relationships of Macroscopic Nuclear Physics* (Springer-Verlag, Berlin, 1988).
[99] A. V. Ignatyuk, *Statistical Properties of Excited Nuclei* [in Russian] (Énergoatomizdat, Moscow, 1983).
[100] Yu. A. Lazarev, I. I. Gontchar, and N. D. Mavlitov, Phys. Rev. Lett. **70**, 1220 (1993).
[101] P. Fröbrich and J. Marten, Z. Phys. A **339**, 171 (1991).
[102] P. Fröbrich, Phys. Rep. **116**, 337 (1984).
[103] M. Blann, Phys. Rev. C **21**, 1770 (1980).
[104] J. E. Lynn, *Theory of Neutron Resonance Reactions* (Clarendon Press, Oxford, 1968), p. 325.
[105] V. G. Nedorezov and Yu. N. Radyuk, *Photofission Beyond the Giant Resonance* [in Russian] (Naukova Dumka, Kiev, 1989).
[106] H. Rossner, Private communication (1992).
[107] A. J. Sierk, Phys. Rev. C **33**, 2039 (1986).
[108] B. B. Back *et al.*, Phys. Rev. C **32**, 195 (1985); **33**, 385 (1986).
[109] F. Videbaek *et al.*, Phys. Rev. C **15**, 954 (1977).
[110] E. Vulgaris, L. Grodzins, S. G. Steadman, and R. Ledoux, Phys. Rev. C **33**, 2017 (1986).
[111] T. Murakami *et al.*, Phys. Rev. C **34**, 1353 (1986).
[112] J. O. Newton *et al.*, Nucl. Phys. A **483**, 126 (1988).
[113] J. Blocki *et al.*, Ann. Phys. (N.Y.) **113**, 330 (1978).
[114] D. J. Hinde *et al.*, Phys. Rev. C **45**, 1229 (1992).
[115] R. J. Charity *et al.*, Nucl. Phys. A **457**, 441 (1986).
[116] J. U. Andersen *et al.*, K. Dan. Vidensk. Selsk. Mat.-Fys. Medd. **40**, No. 7 (1980).
[117] J. van der Plicht *et al.*, Phys. Rev. C **28**, 2022 (1983).
[118] A. Gavron *et al.*, Phys. Rev. C **30**, 1550 (1984).
[119] N. Carjan, Workshop on Open Problems in Heavy Ion Reaction Dynamics at Vivitron Energies, May 5–7, 1993, CRN 93–22, CRN, Strasbourg, p. 524.
[120] H. Rossner *et al.*, Phys. Rev. C **45**, 719 (1992).
[121] G. I. Kosenko, *Candidate's Dissertation* [in Russian] (Tomsk, 1992).
[122] K. Hartel, *Dissertation* (Technische Universität, Munich, 1985).
[123] G. G. Chubaryan *et al.*, Yad. Fiz. **56**, No. 3 (1993) [Phys. At. Nucl. **56**, 286 (1993)].
[124] I. I. Gontchar, Yu. A. Lazarev, and N. D. Mavlitov, "Heavy ion physics," Scientific Report (1989–1990), E7-91-75, JINR, Dubna (1991), p. 70.
[125] I. I. Gonchar, Yu. A. Lazarev, and N. D. Mavlitov, "Heavy ion physics," Scientific Report (1989–1990), E7-91-75, JINR, Dubna (1991), p. 72.
[126] D. Hilscher, I. I. Gontchar, and H. Rossner, Yad. Fiz. **57**, 1255 (1994) [Phys. At. Nucl. **57**, 1187 (1994)].
[127] I. I. Gontchar, P. Fröbrich, and Yu. A. Lazarev, 2nd Int. Conf. on Dynamical Aspects of Nuclear Fission, June 14–18, 1993, Smolenice, Slovakia; E7-94-19, JINR, Dubna (1994), p. 198.
[128] M. Thoennessen *et al.*, Phys. Rev. Lett. **59**, 2860 (1987).
[129] R. Butsch *et al.*, Phys. Rev. C **44**, 1515 (1991).
[130] I. Dioszegi *et al.*, Phys. Rev. C **46**, 627 (1992).
[131] D. J. Hofmann, Ninth Winter Workshop on Nuclear Dynamics, Key West, Florida, January 30–February 6, 1993, preprint.
[132] K.-T. Brinkmann *et al.*, Phys. Rev. C **50**, 309 (1994).
[133] H. van der Ploeg *et al.*, Phys. Rev. Lett. **68**, 3145 (1992).
[134] J. D. Molitoris *et al.*, Phys. Rev. Lett. **70**, 3145 (1993).
[135] J. P. Lestone, Phys. Rev. Lett. **70**, 2245 (1993).
[136] J. P. Lestone *et al.*, Nucl. Phys. A **559**, 277 (1993).
[137] H. J. Krappe and V. V. Pashkevich, Phys. Rev. C **47**, 1970 (1993).
[138] C. Gregoire, H. Delagrange, K. Pomorski, and K. Dietrich, Z. Phys. A **329**, 497 (1988).
[139] H. Ikezoe *et al.*, Nucl. Phys. A **538**, 299 (1992).
[140] H. Ikezoe *et al.*, Phys. Rev. C **42**, 342 (1990).
[141] H. Ikezoe *et al.*, Phys. Rev. C **42**, R1187 (1990).
[142] F. P. Hessberger, V. Ninov, and U. Spoerel, Z. Phys. A **340**, 171 (1991).
[143] L. C. Vaz *et al.*, Z. Phys. A **315**, 169 (1984).
[144] E. Strumberger, K. Dietrich, and K. Pomorski, Nucl. Phys. A **502**, 523c (1989).
[145] V. P. Aleshin, Izv. Akad. Nauk SSSR, Ser. Fiz. **52**, 81 (1988).
[146] V. P. Aleshin, *Doctoral Dissertation* [in Russian] (Kiev, 1991).
[147] D. J. Hofmann, Private communication (1992).
[148] D. Drechsel, *Proc. of the Fourth Seminar on Electromagnetic Interactions of Nuclei at Low and Medium Energies*, December 13–15, 1977, Moscow, USSR (Nauka, Moscow, 1979), p. 293.
[149] J. S. Forster *et al.*, Nucl. Phys. A **464**, 497 (1987).
[150] S. A. Karamyan, Yu. V. Melikov, and A. F. Tulinov, Sov. J. Part. Nucl. **4**, 196 (1973).
[151] W. M. Gibson, Ann. Rev. Nucl. Sci. **25**, 465 (1975).
[152] V. N. Bugrov and S. A. Karamyan, Yad. Fiz. **40**, 857 (1984) [Sov. J. Nucl. Phys. **40**, 546 (1984)].
[153] S. Yu. Platonov, O. V. Fotina, and O. A. Yuminov, Nucl. Phys. A **503**, 461 (1989).
[154] V. N. Bugrov and S. A. Karamyan, Yad. Fiz. **35**, 558 (1982) [Sov. J. Nucl. Phys. **35**, 322 (1982)].
[155] V. N. Bugrov, V. G. Vinogradov, and S. A. Karamyan, Yad. Fiz. **44**, 1389 (1986) [Sov. J. Nucl. Phys. **44**, 903 (1986)].
[156] D. J. Hinde, D. Hilscher, and H. Rossner, Nucl. Phys. A **502**, 497 (1989).

Translated by Julian B. Barbour